

Three-Dimensional Differences in Joint Loads and Muscle Geometries Between Craniofacial Types

Tylor Brekke, DMD

A thesis submitted in partial fulfillment for the
Degree of Master of Science in Orthodontics

Oregon Health & Science University
Portland, OR

2020

Three-Dimensional Differences in TMJ Loads and Muscle Geometries Between Craniofacial
Types

Tylor Brekke, DMD

Master of Science in Orthodontic Research Advisory Committee:

Signature: _____ Date: _____

Jeffrey Nickel, PhD, DMD, MSc
Professor Provisional, Graduate Program Director
Department of Orthodontics
Oregon Health & Science University

Signature: _____ Date: _____

Laura Iwasaki, PhD, DDS, MSc
Professor, Chair
Department of Orthodontics
Oregon Health & Science University

Signature: _____ Date: _____

Ying Wu, PhD, DDS, MSD
Assistant Professor
Department of Integrated Biomedical & Diagnostic Services
Oregon Health & Science University

ACKNOWLEDGEMENTS

First and foremost a big thank you to my thesis committee for all their help in completing this study and thesis. I would never have been able to complete this project without their support and guidance along the way!

Thank you to Ying Liu for all her statistics work that we were very grateful to have.

Thank you to Anahita Javadpour for her assistance with data collection.

And last but most certainly not least is a huge thank you to all of my co-residents, friends and family who have gave me endless support over the years.

TABLE OF CONTENTS

LIST OF TABLES.....	5
LIST OF FIGURES.....	6
ABSTRACT.....	9
INTRODUCTION.....	11
MATERIALS & METHODS.....	23
RESULTS.....	33
DISCUSSION.....	45
CONCLUSIONS.....	50
REFERENCES.....	52
APPENDIX.....	55

LIST OF TABLES

Table 1: Numbers of subjects and Frankfort horizontal mandibular plane angle (FHMPA, mean \pm standard deviation) for two diagnostic groups.

LIST OF FIGURES

Figure 1: Lateral cephalometric imaging of extreme facial types demonstrating differences in the mandibular plane angles (MPA).

Figure 2: Lateral cephalometric imaging of extreme facial types.

Figure 3: Geometry files consisted of coordinates of TMJs, jaw muscles and teeth relative to *x*-axis, *y*-axis and *z*-axis.

Figure 4: Labelled landmarks on lateral (left, showing outlines of the mandibular first molar and central incisor) and posteroanterior (right, showing outlines of condyles) cephalographs.

Figure 5: (BM109) A graphic example of measured and predicted eminence shapes, where the differences between predicted and measured was greater than 0.5mm over 0 to 4 mm of mandibular protrusion.

Figure 6: Differences between the predicted eminence form and the right (red) and left (green) measured eminence form.

Figure 7: Sex and diagnostic group differences in masseter orientation as related to the occlusal plane.

Figure 8: Sex and diagnostic group differences in temporalis orientation as related to occlusal plane.

Figure 9: Diagnostic group differences in female ipsilateral temporomandibular joint (TMJ).

Figure 10: Diagnostic group differences in male ipsilateral temporomandibular joint (TMJ) loads.

Figure 11: Diagnostic group differences in female contralateral temporomandibular joint (TMJ) loads.

Figure 12: Diagnostic group differences in male contralateral temporomandibular joint (TMJ).

Figure 13: Overall sex and diagnostic group (D=dolichofacial; B=brachyfacial) differences in temporomandibular joint (TMJ) loads as percent of bite force.

Figure 14: Overall sex differences in temporomandibular joint (TMJ) loads as percent of bite force.

Figure 15: Overall diagnostic group differences in temporomandibular joint (TMJ) loads as percent of bite force.

Figure 16: Power analysis of data.

Three-Dimensional Differences in Joint Loads and Muscle Geometries Between Craniofacial Types

Tylor Brekke, DMD^a

Jeffrey Nickel, PhD, DMD, MSc^b

Laura Iwasaki, PhD, DDS, MSc^c

Ying Wu, PhD, DDS, MSD^d

^aResident, Department of Orthodontics, Oregon Health & Science University, Portland, OR

^bProfessor Provisional, Graduate Program Director, Department of Orthodontics, Oregon Health & Science University, Portland, OR

^cProfessor, Chair, Department of Orthodontics, Oregon Health & Science University, Portland, OR

^dAssistant Professor, Department of Integrated Biomedical & Diagnostic Services, Oregon Health & Science University, Portland, OR

Keywords: temporomandibular joint, joint loads, muscle geometry, masseter, temporalis, loading force

ABSTRACT

Title:

Three-Dimensional Differences in TMJ Loads and Muscle Geometries Between Craniofacial Types

Objectives:

The objectives of this study were to evaluate for differences in (i) three-dimensional masticatory muscle orientations, and (ii) temporomandibular joint loads, between men and women with brachyfacial and dolichofacial morphologies.

Materials and Methods:

One-hundred and forty-seven subjects completed study protocols. Fifty-seven subjects were included in this study based on access to (i) lateral and anteroposterior cephalometric or cone beam computed tomography (CBCT) imaging, (ii) jaw tracking recordings, and (iii) Frankfort Horizontal-Mandibular Plane (FHMPA) angles of $\leq 22^\circ$ (brachyfacial) and $\geq 28^\circ$ (dolichofacial). Subjects were excluded based on (i) multiple missing or decayed teeth, (ii) pregnancy, (iii) presence of systemic rheumatological or musculoskeletal disease, (iv) degenerative disease of the TMJ or history of TMJ trauma, (v) large dental restorations, (vi) fixed orthodontic appliances, or (vii) claustrophobia. Subjects had an intraoral examination, and either video or dynamic stereometry imaging performed to capture in vivo sagittal eminence shape. Geometry files were developed using lateral and posteroanterior cephalometric landmarks of the condyles, dentition and insertion and origin of the masticatory muscles. A computer driven numerical model used each subject's geometry file to predict the sagittal eminence shape that was consistent with the objective of minimization of joint loads. The predicted and in vivo eminence shapes were compared using a computer program. Small adjustments were made to each subject's geometry file until differences between predicted and measured eminence shapes was ≤ 0.5 mm over 0 - 4 mm of mandibular protrusion. Temporomandibular joint loads for each subject were calculated using their geometry and in vivo eminence data in a numerical model, which used minimization of muscle effort as an objective. Ipsilateral and contralateral joint loads were expressed as a percentage of a 100-unit biting force. Static right canine biting forces were modelled over a comprehensive range of angles. Statistical analyses of the dependent variable of TMJ load used analysis of variance (ANOVA) and Tukey's honest significant difference (HSD) posthoc tests. Independent variables were sex (female, male), craniofacial group (dolichofacial, brachyfacial), biting angle (posteromedial, posterolateral, overall), and TMJ (ipsilateral, contralateral). Similarly, the dependent variable of the angulations of the masticatory muscles was compared via ANOVA and Tukey's HSD posthoc tests where the independent variables were sex (male, female), craniofacial group (dolichofacial, brachyfacial), muscle (masseter, temporalis) and angle (sagittal, coronal). Significance was defined by a p value < 0.05 .

Results:

De-identified data from 57 subjects, 35 females and 22 males, were analyzed. The brachyfacial subjects (16 female, 12 male) had an average FHMPA of $18.2^\circ \pm 2.8^\circ$. The dolichofacial group (19 females, 10 males) had an average FHMPA of $31.9^\circ \pm 4.5^\circ$. There were no statistically significant findings with respect to sex or craniofacial group differences in temporalis muscle geometries. Dolichofacial subjects exhibited generally larger sagittal and coronal angulations of the masseter muscle. In dolichofacial males, the masseter muscle sagittal ($63.9^\circ \pm 8.9^\circ$) and coronal ($38.8^\circ \pm 14.2^\circ$) angles were larger compared to sagittal ($57.7^\circ \pm 7.0^\circ$) and coronal ($30.9^\circ \pm$

5.3°) angles of brachyfacial males, but these craniofacial group differences were not statistically significant (sagittal angle $p=0.085$; coronal angle $p=0.091$). There were no muscle geometry differences between dolichofacial and brachyfacial females. Within the dolichofacial group, the average male sagittal masseter angle of $63.9^\circ \pm 8.9^\circ$ was significantly larger than in female subjects ($54.2^\circ \pm 10.5$, $p=0.019$). Similarly, the average male masseter coronal angulation ($38.8^\circ \pm 14.2^\circ$) was significantly larger ($p=0.012$) compared to females ($27.8^\circ \pm 7.9^\circ$). There were no muscle geometry differences between brachyfacial males and females. With respect to TMJ loads, average TMJ loads of the males ($101.31 \pm 5.1\%$) were significantly ($P<0.01$) larger than females (85.6 ± 28.4). Between craniofacial groups, average loads in dolichofacial subjects ($96.0 \pm 42.8\%$) were significantly higher ($p=0.018$) compared to the brachyfacial subjects ($87.1\% \pm 28.1$). Within craniofacial groups, there were no statistically significant sex differences in TMJ loads. A power analysis with the most stringent criteria showed the need for sample sizes of 73 dolichofacial and 73 brachyfacial subjects to detect statistically significant differences in ipsilateral and contralateral TMJ loads between men and women, and between craniofacial groups.

Conclusions:

Hypothesis 1: There were no differences in ipsilateral, contralateral, and overall TMJ loads between brachyfacial and dolichofacial individuals

- a) Dolichofacial subjects had significantly higher average TMJ loads than brachyfacial subjects.
- b) Between diagnostic groups, there were no sex differences in TMJ loads.

Hypothesis 2: There were no sex differences in ipsilateral, contralateral, and overall TMJ loads during static canine biting conditions.

- c) Male subjects had significantly higher average joint loads compared to females.
- d) Within diagnostic groups, although males had higher ipsilateral and contralateral TMJ loads compared to females, differences were not statistically significant.
- e) Within diagnostic groups, although males had higher ipsilateral and contralateral TMJ loads compared to females, differences were not statistically significant.

Hypothesis 3: There were no differences in the sagittal and coronal angulations of the masseter or temporalis muscles between brachyfacial and dolichofacial groups.

- a) Dolichofacial males exhibited larger, and near statistically significant, sagittal and coronal angulations compared to brachyfacial males.
- b) There were no statistically significant differences in muscle geometries between dolichofacial and brachyfacial women.

Hypothesis 4: There were no differences in the sagittal and coronal angulations of the masseter or temporalis muscles between female and male subjects.

- c) There were statistically significant difference in masseter muscle geometry between dolichofacial men and women.
- d) No statistically significant differences were found in masseter angulations between brachyfacial men and women.
- e) No statistically significant sex or diagnostic group differences were found for temporalis muscle geometry.

INTRODUCTION

A. CRANIOFACIAL GROWTH PATTERNS

The growth and development of the craniofacial complex is a complicated and multifactorial process. Understanding the variable growth patterns of patients has been a long-standing goal in orthodontics. Classification of skeletal extremes has lacked consensus amongst orthodontists historically. Terminology has varied because diagnostic criteria have varied.¹ Commonly accepted terms to classify facial types include brachyfacial, mesofacial and dolichofacial which are usually defined by their Frankfort horizontal mandibular plane angle (FHMPA) (Figure 1). The corresponding FHMPAs are brachyfacial $\leq 22^\circ$; mesofacial $22-28^\circ$; dolichofacial $\geq 28^\circ$.

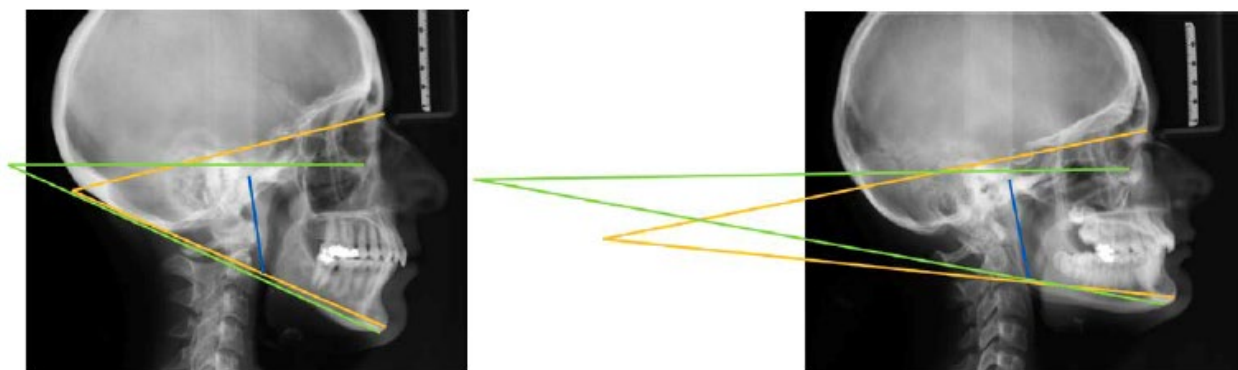


Figure 1: Lateral cephalometric imaging of extreme facial types demonstrating differences in the mandibular plane angles (MPA). Nasion-Sella:Gonion-Gnathion (yellow) and Frankfort Horizontal:Gonion-Gnathion (green) quantified the MPA. Mandibular ramal height is measured from the top of the condyle to Gonion (blue). A Dolichofacial phenotype (left) has relatively larger mandibular plane angles (yellow and green) and shorter ramal height (blue). The Brachyfacial phenotype (right) has smaller mandibular plane angles (yellow and green) and a longer ramal height (blue).²

The extreme facial patterns also differ with respect to anterior facial height (AFH) proportions. The lower AFH (LAFH, anterior nasal spine to menton) is relatively short and long compared to the total AFH (TAFH, nasion to menton) in brachyfacial and dolichofacial types, respectively (Figure 2).

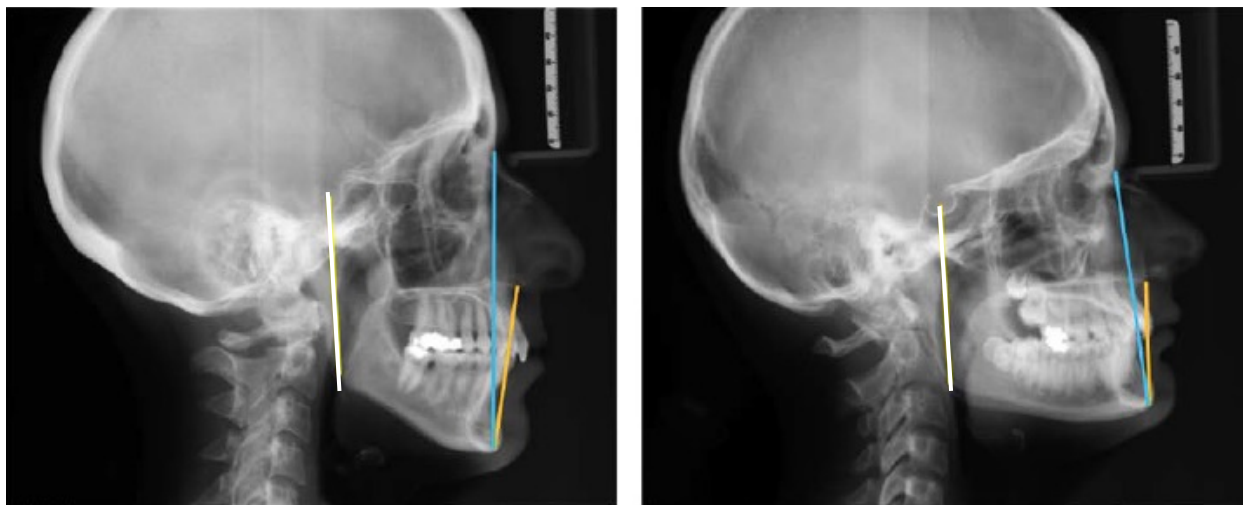


Figure 2: Lateral cephalometric imaging of extreme facial types. In the Dolichofacial phenotype (left) the lower anterior facial height (orange) is longer compared to total anterior facial height (blue). Brachyfacial type (right) has a proportionally smaller lower anterior facial height (orange) compared to total anterior facial height (blue). Lower Anterior Facial Height (LAFH), is measured from Anterior Nasal Spine to Menton (ANS-Me, orange); Total Anterior Facial Height (TAFH) is measured from Nasion to Menton (Na-Me, blue).²

Alternative terms for brachyfacial include short-face syndrome and hypodivergence; while alternative terms for dolichofacial include long-face syndrome and hyperdivergence. All terms have some form of cephalometric-based measurement categorization. Longitudinal research has shown that individuals in the extreme facial growth patterns tend to hold to these patterns throughout maturity.³ Such patterns dictate the overall growth direction of the craniofacial complex.

It has been proposed that the temporomandibular joint (TMJ) develops with the objective function to minimize joint loads and/or minimization of muscle effort. The effects of joint loading may alter condylar growth and eminence form.^{4 5} It is possible however that variable joint loads induced through custom oral appliances, may be able to alter this pattern and affect TMJ growth and ultimately achieve a more harmonious growth pattern. If joint loads in the TMJ

that lead to favorable growth patterns could be known, then these could possibly be imposed therapeutically in individuals with unfavorable growth patterns to correct them.

Much of the variation in face height between facial types can be attributed to the growth of the mandible at the condyle. Bjork showed in his implant studies that the amount of the condylar growth was strongly correlated with the forward-downward rotation of the mandible during growth and also significantly, but less so, with the rotation of the maxilla as well.⁶ However, single morphological measurements at one time-point are not sufficient to describe comprehensively the overall growth of the craniofacial complex.

The craniofacial growth processes are dynamic longitudinally and regionally different in amount and timing. Therefore, it is important to understand the beginning, peaks, and cessation of growth in each component to intervene appropriately with growth modification techniques. For example, the mandible tends to grow more and later compared to the maxilla and there are known sex differences.⁷ Growth of the craniofacial complex seems to be dependent on both hereditary transmission and environmental factors. The genetic component can be visualized through the uncanny similarities and correlations of growth through familial tendencies. The environmental factors such as diet and nutrition, level of masticatory function, and speech may not be as vivid due to the slow progressive affects they have over the long-spanning development process. Studying individuals, not averages, and their growth patterns it seems there are differences in the relative rates of growth in the vertical, anterior and posterior dimensions temporally. There is a tendency for the jaws and face to grow downward and forward relative to the cranial base but the relative amounts vary amongst individuals.

With the introduction of clinical cephalometrics in the 1940s, orthodontists began to develop a better understanding of the underlying skeletal disproportions in the etiology of certain

malocclusions. Historically the identification of skeletal relations was used more for diagnostic purposes than treatment planning. Diagnosis of moderate to severe skeletal disproportions gave justification for orthodontic camouflage treatment modalities albeit with compromised results. There was little that could be offered to treat such skeletal discrepancies until 30 years later in the 1970s.⁸ Advancements in orthognathic surgical approaches and imaging techniques allowed orthodontists in conjunction with the oral surgeons to correct more predictably and esthetically patients with moderate-severe skeletal disproportions and their underlying malocclusions. With these new advances, quantifying cephalometric norms and their variations became the standard of care.

Historically, the work of many orthodontists advanced cephalometric analyses and their applications. With development of cephalometric diagnostic parameters, many diagnostic terms and definitions were introduced. Initial classifications of extreme vertical skeletal discrepancies were based on the open-bite and deep bite presentations.⁹ The variation of these two presentations was mostly attributed to the variability in mandibular ramus height (Figure 1).^{9,10} Individuals with relatively large mandibular ramus heights tended to have small gonial angles, increased hinged rotational closing of the mandible and associated deep overbites as seen in brachyfacial individuals. The opposite is true for dolichofacial individuals with small mandibular ramal heights who tended to have large gonial angles and anterior open bites. Using the mandibular ramus height as the key diagnostic measurement was disputed by Fields et al., who found that the mandibular ramus height was not an ideal indicator of skeletal discrepancy alone, because the craniofacial complex relies on many factors in harmony to create an esthetic balance.¹¹ That is, no single parameter is sufficient in itself to identify accurately a given facial type.^{11,12}

It has been shown that dolichofacial or high mandibular plane to sella nasion angle (MP:SN) subjects have small amounts of vertical condylar growth and proportionally large amounts of vertical alveolar and sutural growth.¹³ This leads to the clockwise rotation of the mandible, long lower anterior face height (LAFH) and short posterior ramus height.¹³ On the contrary, subjects with low MP:SN angles tend to have relatively large amounts of vertical condylar growth, longer ramus heights, decreased LAFH and a forward rotation of the mandible bringing pogonion anteriorly.¹³ Investigators including Bishara, Jakobsen, Siriwat, Jarabak and many others added to the list of defining characteristics shown amongst these cohorts of variable facial growth patterns.^{14,15}

B. MECHANICS OF MANDIBULAR GROWTH

Primary growth of the mandible takes place in the condyle through the process of chondrogenesis followed by ossification. This growth contributes to an increase in the ramal height of the mandible. While growth of the maxilla and posterior alveolar components of both jaws affect the vertical dentofacial relations.¹⁶ Typical growth of the condyle relative to the chin and lower border of the mandible occurs in the anterosuperior and posterior directions.¹⁷ Through the development of occlusion, masticatory requirements due to diet, and other jaw functions, there are variations in joint loads within individuals over time and between individuals. The mechanical loading of the condyle and eminence stimulate condylar growth and affect facial growth pattern.^{17,18}

The growth in the shape of the condyle differentially favors mediolateral over anteroposterior growth. The anteroposterior condylar changes are relatively minimal throughout development compared to the approximate doubling of the mediolateral dimension.¹⁹ The stress fields, or stress distributed over a given area of contact, induced between the condyle and articular

eminence may be in part responsible for this variable growth pattern. It appears that areas of high shear strain promote osteogenesis and inhibit chondrogenesis.²⁰ If so, higher anteroposterior than mediolateral shear strains occur in the TMJ during jaw functions and consequently differentially inhibit chondrogenesis in the anteroposterior dimension but promote it the mediolateral dimension, this could explain shape changes in the condyle from birth to maturity. In vivo measurements of these TMJ shear strains, stress field movements and other variables such as the energy densities, or energy applied to the system during function per unit volume of tissue, as well as tissue hypoxia or solute diffusivities, may help elucidate the underlying mechanisms, affecting chondrogenesis, osteogenesis and TMJ tissue repair.²¹ More research in this area is required. However, it is known that the loading of the mandible and TMJ apparatus is necessary for growth and development of the mandible and eminence.²² If the joint loads are decreased then variable expressions of growth factors limit vertical growth. This leads to a decreased posterior face height due to a decreased ramal height and tendency towards the dolichofacial pattern.²³

Currently the precise range of strain or energy densities within the TMJ required to promote condylar growth are unknown. By identifying these naturally occurring joint loads in variable facial types the range of loading for mesofacial development could be better understood. The condyle is comprised of four cell layers: fibrous, proliferative, chondrocytic and hypertrophic layers. The mechanical forces within the condyle regulate gene expression and control whether the cells within the proliferative region differentiate to osteoblast or chondrocytes.¹⁷ Functional appliances currently used induce differential growth of the jaws in certain individuals.²⁴ Primate studies have confirmed this through histological evidence of condylar growth center responses to functional therapy²⁵ where the mandible was postured forward and possibly changed the

congruency of the TMJ hard tissues, resulting in changes in joint loads. A main challenge for functional appliance therapy is that outcomes are unpredictable in terms of induction of mandibular growth. When functional appliances are used currently, the effects on joint load magnitudes are expected to be changed because of altered orientations of muscle of mastication and relative positions of joint components, but by how much is unknown. Not knowing the magnitude and frequency of these loads during functional appliance therapies might explain the variable clinical outcomes. There is a need for more quantitative and defined clinical guidelines for the use of functional appliances, and their variable joint loading effects.

C. CURRENT TREATMENT MODALITIES FOR VARIABLE GROWTH PATTERNS

There are a multitude of appliances available, but a better understanding of how these appliances function and the forces they induce on the temporomandibular apparatus may shed light as to why they are so successful, or not, in different individuals. The differences in facial type, and associated growth trajectory, are critical in diagnosis and treatment planning but measuring morphology does not explain mechanisms. While it has been shown that individuals with variable skeletomuscular growth patterns express varying responses to a given treatment modality²⁶ and certain malocclusions and facial esthetics may change the expected prognosis, a better understanding of jaw mechanics and behaviors could improve predictability of dentofacial orthopedics.

The two primary approaches to treating skeletal discrepancies are functional appliances for growth modification in children and orthognathic surgery in adults. Mild to moderate vertical discrepancies may not be as apparent as transverse or anteroposterior disharmonies in childhood. This is likely due to the vertical component of growth being the last to complete, following both growth in the transverse and anterior-posterior dimensions.²⁷ The effects of the vertical

dimension in orthodontic treatment can be greatly magnified due to the hinge-like TMJ. Minor changes in the posterior vertical dimensions can exhibit great changes in the anterior occlusion. For example, brachyfacial deep-bite individuals may be treated by increasing the vertical dimension of the occlusion with an appliance covering the anterior dentition to allow the posterior dentition to continue to erupt and, thus, decrease the anterior overbite. However, dolichofacial individuals with anterior open bite tendencies should not be treated the same way and increasing the vertical dimension of occlusion needs to be avoided to not worsen the open bite and increase the MPA. On the other hand, functional appliances with posterior occlusal coverage for posterior dental intrusion may be indicated in dolichofacial, but not brachyfacial patients. When mandibular growth is desired to correct a skeletal malocclusion, current functional appliance therapy on average offers in the range of 0-3 degrees of ANB correction²⁴ and it is impossible to know what portion of the outcome is due to the appliance versus normal growth. In functional appliance studies it is often difficult to determine whether or not the individual's favorable growth change with the use of a functional appliance, would have occurred without the use of such appliance due to lack of control subjects for comparison. Although functional appliances seem to contribute to successful treatment of some growing children, the mechanisms that account for their variable effectiveness in different craniofacial types are poorly understood.²¹

In adults, altering growth trajectory of the jaws is no longer an option. Surgical approaches however have improved dramatically over the last 50 years. For dolichofacial non-growing individuals where surgery is indicated, the treatment of choice is typically maxillary impaction. This reduces the height of the maxillary posterior occlusion allowing the mandible to close to a decreased vertical dimension, thus, reducing the mandibular plane angle, decreasing the lower

anterior face height and often times improving anterior-posterior disharmonies.¹¹ Individuals with brachyfacial features and a deep overbite are often more reliably treated with traditional orthodontic modalities. However, in more severe skeletal discrepancies either mandibular advancement or combined maxillo-mandibular surgery may be used to correct the jaw relations and malocclusion. Surgery can be an appropriate alternative for those individuals who were not afforded early orthodontic intervention or whose skeletal disharmony was not diagnosed as a child. Orthognathic surgeries to correct malocclusions are costly and carry significant risks of morbidity. Reliably and consistently correcting aberrant growth patterns with functional appliances would reduce the future need for such corrective surgeries and greatly reduce the overall expenses and risks.

D. DIAGNOSTIC GROUP DIFFERENCES IN TMJ LOADING

Recent research using three-dimensional numerical modeling algorithms have shed some light on sex and craniofacial phenotype differences in TMJ loads and energy densities.^{2,28,29} A recent clinical study²⁸ comparing eighteen adult females and eighteen adult males looked at ipsilateral and contralateral TMJ loads and energy densities, or energy applied to the joint system per unit volume of tissue (mm^3), during jaw closing. The male and female subjects generally showed higher TMJ loads in the contralateral compared to the ipsilateral TMJ, but no statistically significant overall TMJ load differences between females (16.3 ± 4.2 N) and males (15.7 ± 2.6 N). However, they concluded that females demonstrated significantly larger mean energy densities of the TMJ for the same jaw closing task as compared to males. The mean energy densities per closing cycle for ipsilateral and contralateral TMJs were $9.0 (\pm 9.6)$ and $8.4 (\pm 5.5)$ mJ/mm^3 for females, and $5.6 (\pm 4.2)$ and $6.3 (\pm 4.2)$ mJ/mm^3 for males respectively. That is, the TMJ energy densities on the ipsilateral and contralateral sides were 38% and 25% larger,

respectively, in females compared to males.²⁸ This may in part explain the reason higher levels of joint degeneration and temporomandibular disorders (TMDs) have been reported in females than males.

Nickel et al.² evaluated the mechanobehavior in dolichofacial ($MP-SN \geq 37^\circ$) and brachyfacial ($MP-SN \leq 27^\circ$) adolescents. Their objectives were to identify differences in TMJ loads and muscle use between different facial types and to evaluate if there was any correlation with ramus height. Dolichofacial subjects had significantly higher TMJ loads when compared to brachyfacial subjects with the ipsilateral TMJ loads in the dolichofacial subjects being $\geq 20\%$ larger for some biting angles. There was also a significant relationship amongst normalized TMJ loads and ramus height with the mean dolichofacial and brachyfacial ramus heights measuring 50 ± 4 mm and 54 ± 4 mm respectively. They also showed that brachyfacial individuals showed higher frequencies of low-level muscle activation. Dolichofacial individuals displayed significantly less masseter (day, night) and temporalis (night) duty factors, which are measures of the percentage of time a muscle is active during the overall electromyography recording time.

E. TMJ EMINENCE MODELING

Three-dimensional modeling algorithms have been developed using muscle geometry files to predict the sagittal eminence shape. These model predictions assumed that the eminence shape develops under the objective function of minimization of joint loads, and was a unique outcome of the growth and remodeling responses to TMJ loads. Magnitudes of TMJ load depend on an individual's anatomy, including the three-dimensional position and orientation of the masticatory muscles, and positions of the teeth and TMJs.^{4,30,31} The sagittal eminence shape was developed from model-predicted TMJ loads for a series of biting positions as the mandible moves from an maximum intercuspation, to protrusive position with the jaw centered symmetrically. The model

predicted both the TMJ loading magnitudes and directions. In order for the relatively frictionless TMJ structures to be static during biting, the joint loads were expected to be directed perpendicular to the opposing (right and left eminence) surfaces. Hence, a series of surfaces, each perpendicular to the TMJ loading directions for the series of biting positions from maximum intercuspation to protrusion, comprised the sagittal eminence shape.^{4,30,32}

Current numerical models have assumed symmetry between the right and left eminences. In vivo, effective sagittal eminence shape has been defined as the sagittal plane trajectory of the TMJ stress-field during symmetrical protrusion and retrusion.^{3,34} Jaw tracking methods⁵ have been used to measure, in vivo, sagittal eminence shapes, which have been compared to model-predicted eminence shapes for individuals. These model predicted shapes, based on an objective of minimization of joint loads, have been confirmed to predict the eminence shape on at least one side. The average reported error was $\leq 17\%$.⁵ To date, a numerical model that can accurately predict asymmetrical eminence forms, is currently unavailable. Development of such a model may prove to be beneficial in future research.

F. MODELING OF TMJ LOADS

Studies involving the TMJ have proven quite difficult due to the mechanical indeterminacy. That is, a number of different combinations of jaw muscle activations can be used to accomplish the same biting or other jaw-loading task. Thus, TMJ mechanics can vary on an individual basis depending on the gross anatomy of the TMJ, jaw muscles, biting position and angle, and dentition present. Traditional strategies used average electromyography (EMG) values of muscles of mastication for specific biting conditions to calculate joint loads,^{33,34} but unless the EMG data are individual- and task-specific, these strategies were not likely to result in joint loads that reflected in vivo conditions of a given individual. Newer three-dimensional modeling

programs have been reported which accurately define the boundaries of hard and soft tissue anatomy to predict muscle of mastication activity and joint/eminence loads during variable biting conditions.^{4,30,35} Trainor et al. described an optimization strategy for the neuromuscular control. This was called an objective function.³⁵ In order to achieve a unique numerical modeling solution for muscle forces and joint loads in response to loading of the mandible, an objective function such as minimization of joint loads (MJL) or minimization of muscle effort (MME). These objective functions produced computer predicted data that most closely matched in vivo measured muscle forces for the same jaw-loading tasks,⁴ and have been shown to estimate reliably masticatory muscle forces during static mandibular loading conditions with an average error of <15%.³⁶ More recently, numerical modeling has been shown to predict muscle activation patterns and joint loads which satisfied the objective functions of MJL, MME, or both depending on the individual.^{4,31,35} However, to date, there have been limited studies which compared joint loading mechanics between craniofacial types.

G. Purpose of Research

Differences in three-dimensional muscle geometries of individuals may lead to differences in TMJ loads for the same biting tasks. Differences in joint loads could account for growth differences in mandibular condyle, and differences in articular eminence shapes between dolichofacial and brachyfacial phenotypes. The overall objective of the project was to test if there were differences in joint loads between dolichofacial and brachyfacial individuals which were correlated with three-dimensional differences in masticatory muscle orientation.

H. HYPOTHESES

1. There were no differences in ipsilateral, contralateral, and overall TMJ loads between brachyfacial and dolichofacial individuals
2. There were no sex differences in ipsilateral, contralateral, and overall TMJ loads during static canine biting conditions.
3. There were no differences in the sagittal and coronal angulations of the masseter or temporalis muscles between brachyfacial and dolichofacial groups.
4. There were no differences in the sagittal and coronal angulations of the masseter or temporalis muscles between female and male subjects.

MATERIALS & METHODS

A. POPULATION SAMPLE

Two hundred and forty-two subjects, from two parent projects, were evaluated for inclusion over the dates of September 2006 to June 2008 and November 2011 to February 2014. Subjects were recruited from the University at Buffalo School of Dental Medicine patient population as well as surrounding areas. Informed consents were given by each participant. From a pool of 147 subjects who completed study protocols, de-identified records and data were selected based on access to (i) cephalometric or cone beam computed tomography (CBCT) imaging to create three-dimensional geometry files, and (ii) jaw tracking recordings to derive sagittal eminence shapes.

Study inclusion criteria were based on Frankfort to Mandibular Plane angles (FHMPA). Subjects with $FHMPA \leq 22^\circ$ were included, and were defined as having a brachyfacial pattern. Individuals with $\geq 28^\circ$ FHMPA were defined as having a dolichofacial pattern, and were included in the study. Gender and other demographic data were self-reported and gathered from initial examination documentation. Exclusion criteria were FHMPA of >22 and $<28^\circ$, multiple

missing or decayed teeth, pregnancy, systemic rheumatological or musculoskeletal disease, TMJ degenerative disease based on CBCT imaging, large dental restorations, fixed orthodontic appliances, claustrophobia, and history of TMJ trauma.

B. CLINICAL PROCEDURES

a. CT and CEPHALOMETRIC IMAGING

Subjects had CT imaging (Galileos Comfort, Dentsply Sirona, York PA, USA) which was used by a calibrated examiner to assess TMJ status according to diagnostic criteria for temporomandibular disorders (DC/TMD) Axis I criteria.³⁷ As well, either lateral and posteroanterior cephalometric radiographs, or cephalograms derived from full head CT images were used to aggregate three-dimensional craniomandibular anatomy into geometry files, that was subsequently used in computer driven numerical modeling programs.³⁸ Lateral cephalograms were printed (1:1 scale) for hand tracing by one examiner to determine, based on FHMPA, assignment of subjects to brachyfacial and dolichofacial diagnostic groups. This examiner was blinded to all other diagnostic criteria at time of tracing.

b. CLINICAL EXAM

Intraoral and extraoral clinical examinations were completed for all subjects. Inclusion and exclusion criteria were used to determine whether or not a subject was enrolled in the study. Additionally, a calibrated examiner used DC/TMD Axis I Diagnostic Criteria to determine whether or not the right and left TMJs met inclusion criteria based on absence of degenerative joint disease.³⁹

c. SAGITTAL EMINENCE SHAPE MEASURED IN VIVO

In vivo sagittal morphologies of subjects' eminence shapes were determined by one of two methods. For subjects recruited from September 2006 to June 2008, video capture methodology was used to determine right and left eminence shapes relative to occlusal plane. The video jaw tracking protocol has been previously described, where eminence shapes were quantified using a third order (cubic) polynomial equation.⁵ An alternative method was used for subjects recruited from November 2011 to February 2014. In these subjects, a dynamic stereometry method was used. This technique involved combining magnetic resonance imaging and jaw tracking data to produce an animation of the three-dimensional movement of the right and left TMJ stress-fields. From these data, the in vivo sagittal eminence morphology was characterized using a third order (cubic) polynomial equation.³⁸

C. NUMERICAL MODELING

a. CBCT LANDMARKS FOR GEOMETRY FILES

The geometry files used a predetermined x, y, and z orthogonal axes system (Figure 3). The x axis was anteroposterior in orientation and parallel with the occlusal plane. The y axis was vertical and perpendicular to the occlusal plane. The z axis was transverse in orientation, perpendicular to the x and y axes, and intersected the superior most points of the right and left mandibular condyles. The origin of the axes, with x, y, and z coordinates of 0,0,0 was located equidistant along the z axis from the superior most points on the right and left mandibular condyles (Figure 3).

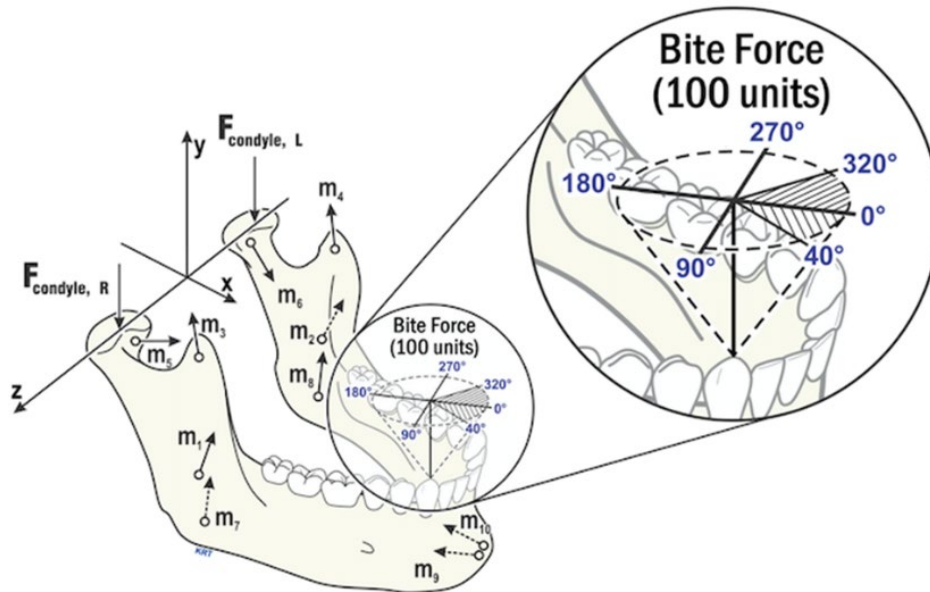


Figure 3: Geometry files consisted of coordinates of TMJs, jaw muscles and teeth relative to x -axis, y -axis and z -axis. Each subject's anatomy determined force vectors for TMJ position ($F_{condyle}$) and jaw muscle position and direction ($m_{1,2}$ =masseter, $m_{3,4}$ =anterior temporalis, $m_{5,6}$ =lateral pterygoid, $m_{7,8}$ =medial pterygoid, $m_{9,10}$ =anterior digastric muscles). Given an applied bite-force (100 units) and biting angle (enlargement right: θ_{XZ} in the occlusal plane and θ_Y where 0° is perpendicular to occlusal plane), the numerical models predicted force vector magnitudes relative to the applied bite-force.²

The geometry files used in the computer generated numerical models were comprised of the x , y , and z coordinates of the mandibular condyles, incisor, canine, molar teeth, and masticatory muscle centroid positions (Figure 3).³⁵ The incisor, canine and molar teeth coordinate locations were determined using lateral and posteroanterior cephalograms (Figure 4, white). Masticatory muscle centroids, defined as the center of muscle areas of attachment and insertion, were identified on lateral and posteroanterior cephalograms (Figure 4) obtained via conventional radiography, or derived from the CBCT images using software (Dolphin®, version 11.95, February 2020, Patterson Dental Supply, Inc., Saint Paul, MN 55120). All skeletal/dental landmarks were determined by study personnel blinded to subject diagnostic group assignment. The masseter sagittal angle (MSA) and temporalis sagittal angle (TSA) were measured by

marking the masseter and temporalis insertion/origin muscle centroids on a lateral cephalogram. The MSA/TSA angles were formed between a line connecting the muscle centroids and a line along the occlusal plane (Figure 4, left). The masseter coronal angle (MCA) and temporalis coronal angle (TCA) were measured in a similar fashion. Using a posteroanterior cephalogram the muscle centroids were located and created a line of action for the masseter and temporalis muscles respectively. The angle was then formed between the muscle centroids and the occlusal plane (Figure 4, right).

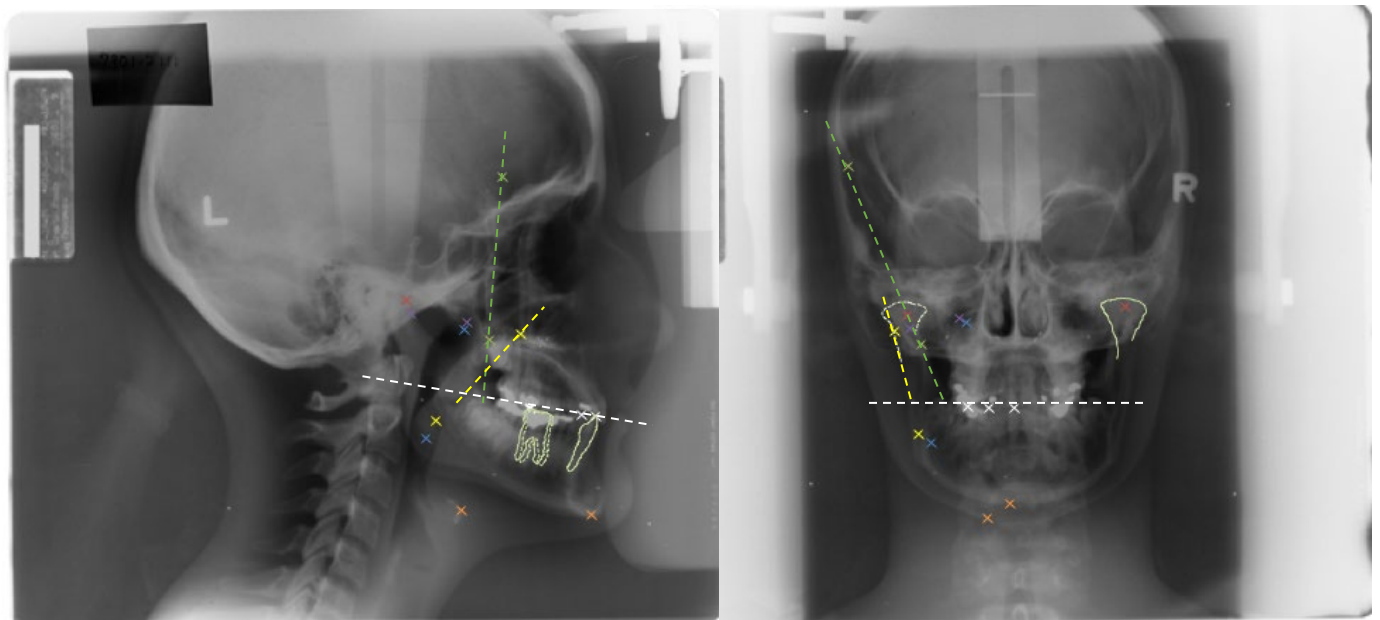


Figure 4: Labelled landmarks on lateral (left, showing outlines of the mandibular first molar and central incisor) and posteroanterior (right, showing outlines of condyles) cephalographs. The identified landmarks are red = condyle; yellow = masseter, green = temporalis, blue = medial pterygoid, purple = lateral pterygoid, orange = digastric muscles; white = teeth (incisor, canine, and molar). Masseter sagittal angle (MSA) lateral cephalogram (left, white and yellow dotted lines). Temporalis sagittal angle (TSA) lateral cephalogram (left, white and green dotted lines). Masseter coronal angle (MCA) posteroanterior cephalogram (right, white and yellow dotted lines). Temporalis coronal angle (TCA) posteroanterior cephalogram (right, white and green dotted lines).⁴⁰

b. EFFECTIVE SAGITTAL EMINENCE SHAPE PREDICTED BY NUMERICAL MODELING

The methods used to produce numerical model predicted TMJ sagittal eminence morphologies have been described previously.^{4,5,32,35} In brief, individual-specific geometry files were used in an eminence creator program which employed an algorithm which optimized solutions to meet the objective of minimizing the sum of right and left TMJ loads. The minimization of joint loads algorithm produced a polynomial equation describing the predicted sagittal morphology of the eminence for the individual. The polynomial equation was a prediction of the eminence shape tracked from a mandibular position of maximum intercuspation (0 mm) to a maximum of 6 mm of mandibular protrusion. The resulting eminence shape predicted by the model was plotted on an axis system where the horizontal axis was 0 – 6 mm of mandibular protrusion, parallel to occlusal plane, and the vertical axis showed the corresponding height of the eminence for 0.5 mm increments of mandibular protrusion. Vertical axis measurements started from 0 mm, where the mandible was in maximum intercuspation position, and increased negatively with mandibular protrusion to the largest negative value (mm) which represented the crest of eminence. The predicted results could then be compared with in vivo data produced by either sagittal view video recordings of mandibular condyle movement, or by dynamic stereometry (Figure 5).

REFINEMENT OF GEOMETRY FILES

An eminence comparison program was used, where each subject's in vivo measured eminence shape and the model predicted eminence shape were compared (Figure 5). If the measured right or left (Figure 5, red and green respectively) eminence shape and predicted eminence shape were ≤ 0.5 mm over 4 mm of mandibular protrusion, no adjustments to the geometry file were necessary. If there were predicted versus in vivo differences of > 0.5 mm over 4 mm of mandibular protrusion, adjustments were made in the anteroposterior (x axis) origin coordinate of the masseter

and, secondarily, temporalis muscles. This protocol allowed for further refinement of the predicted eminence shape from the eminence prediction program. That is, by an iterative process of small changes of x-axis coordinates of the masseter, and secondarily of the temporalis muscle origins, a revised predicted eminence shape was obtained for comparison with the in vivo eminence shape (Figure 6A). This process was iterated until the subject's predicted and measured sagittal eminence shape of either the left or right TMJ matched, according to the criteria of ≤ 0.5 mm differences between predicted and measured shape over 4 mm of mandibular protrusion. All refinements of geometries were reviewed by inspecting radiographic images to confirm that alterations to geometry files were within normal anatomical limits.

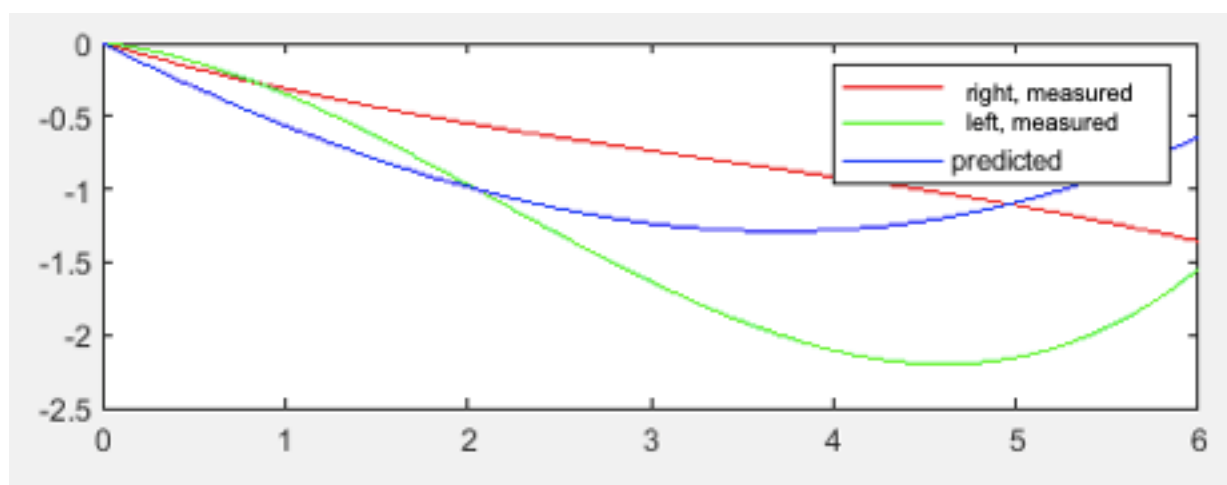


Figure 5: (BM109) A graphic example of measured and predicted eminence shapes, where the differences between predicted and measured was greater than 0.5 mm over 0 to 4 mm of mandibular protrusion. The red and green lines are the polynomials for the measured right and left eminence shapes, respectively, while the blue line is the polynomial for the model-predicted eminence shape. The x-axis represents the amount of mandibular protrusion (millimeters) where 0 = most retruded mandibular position and the y-axis represents the millimeter change in the eminence shape with respect to mandibular protrusion, where $y = 0$ is at the level of the most superior-anterior point on the condyle and parallel to the occlusal plane.

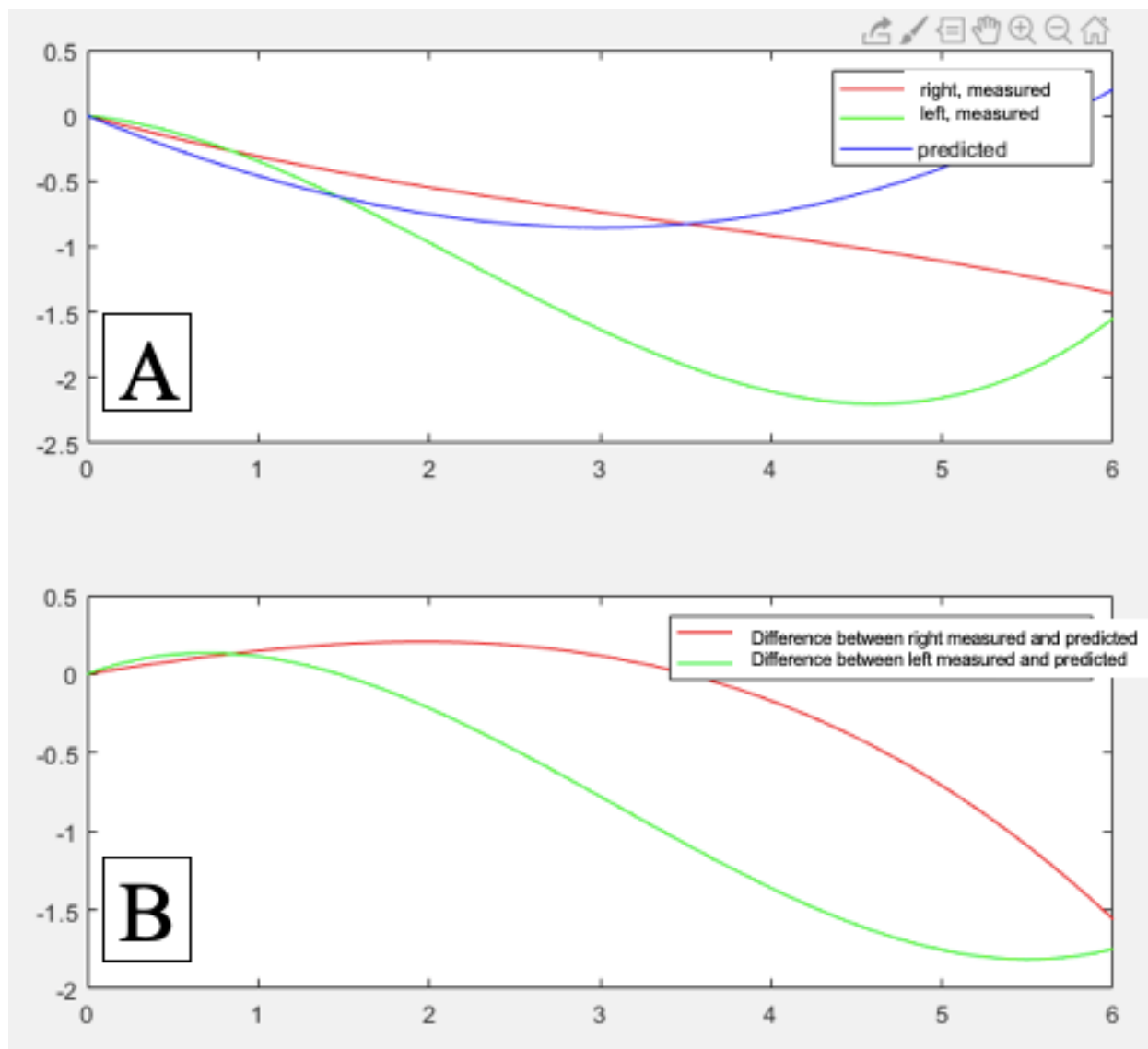


Figure 6A: The initial predicted effective eminence shape (blue) was altered from its original shape seen in Figure 5 (blue) by adjusting the masseter muscle origin x-coordinate by +1.5 mm. This alteration in the geometry file was done to achieve a match between the revised predicted (A, blue) and right measured (A, red) eminence shapes over 0 to 4 mm of mandibular protrusion. The red and green lines are the polynomials for the measured right and left eminence shapes, respectively, while the blue line is the polynomial for the model-predicted eminence shape. The x-axis represents the amount of mandibular protrusion (in millimeters) where 0 = most retruded mandibular position and the y-axis represents the millimeter change in the eminence shape with respect to mandibular protrusion, where $y = 0$ is at the level of the most superior-anterior point on the condyle and parallel to the occlusal plane. Figure 6B: Overall differences between the predicted eminence form and the right (red) and left (green) measured eminence form. The difference between the right measured eminence and the, altered, predicted eminence polynomial are shown in red. The difference between the left measured eminence and the, altered, predicted eminence polynomial are shown in green. The x-axis represents the amount of mandibular protrusion (in millimeters) and the y-axis represents the difference, in millimeters between the measured and

predicted eminence polynomials during mandibular protrusion. The x-axis represents the amount of mandibular protrusion (in millimeters) where 0 = most retruded mandibular position and the y-axis represents the difference (\pm) in the eminence shape with respect to mandibular protrusion, where $y = 0$ is at the level of the most superior-anterior point on the condyle and parallel to the occlusal plane. This graph shows that the right measured and predicted eminence forms now meet the criterion for a match of ≤ 0.5 mm discrepancy out to 4mm of mandibular protrusion.

c. CALCULATIONS OF TMJ LOADS

TMJ loads were determined using a subject's geometry and measured eminence files in a computer-assisted numerical model which predicted TMJ loads and muscle forces based on a neuromuscular objective of minimization of muscle effort.³¹ The geometry file and measured eminence shape file of each participant were used in the model to predict ipsilateral and contralateral TMJ forces, or loads, per unit of bite force (%), for static bite forces of 100 units applied over a range of canine tooth biting angles. That is, static bite forces were applied on the mandibular right canine vertically (Figure 3, $\theta_{xz} = 0$ degrees, $\theta_y = 0$ degrees) and for a range of directions in a plane parallel to the occlusal plane ($\theta_{xz} = 0$ -350 degrees in steps of 10 degrees), and a range of angles relative to a line perpendicular to the occlusal plane ($\theta_y = 0$ -40 degrees in steps of 5 degrees, Figure 3). This approach facilitated the calculations of TMJ loads for a full range of potential biting angles that could occur naturally during jaw functions. Analysis of ipsilateral and contralateral joint loads focused on those in response to canine biting forces which directed the mandible posteriorly ($\theta_{xz} = 0, 360$ degrees), posteromedially ($\theta_{xz} > 0$ -40 degrees) and posterolaterally ($\theta_{xz} < 360$ -320 degrees) (Figure 3) because the bite force angulations on the right mandibular canine load the periodontal ligament and then transmit the forces to the mandible as described. Thus, joint loads were averaged for canine biting over all biting angles modeled, termed "average," and at $\theta_y = 0$ -40 degrees and $\theta_{xz} 360$ to 320 degrees, termed "negative bite force angles," and $\theta_{xz} 0$ -40 degrees, termed "positive bite force angles."

D. DATA AND STATISTICAL ANALYSES

Analysis of the data was undertaken to address the hypotheses as follows:

Hypothesis 1: There were no differences in ipsilateral, contralateral, and overall TMJ loads between brachyfacial and dolichofacial individuals. The dependent variable was TMJ load. The independent variables were (i) craniofacial group (brachyfacial, dolichofacial), (ii) TMJ (ipsilateral, contralateral, overall), and (iii) canine biting angle (positive, negative, and average).

Hypothesis 2: There were no sex differences in ipsilateral, contralateral, and overall TMJ loads during static canine biting conditions. The dependent variable was TMJ load. Independent variables were (i) sex (female, male), (ii) craniofacial group (brachyfacial, dolichofacial), (iii) TMJ (ipsilateral, contralateral, overall), and (iv) canine biting angle (positive, negative, and average).

Hypothesis 3: There were no differences in the sagittal and coronal angulations of the masseter or temporalis muscles between brachyfacial and dolichofacial groups. Dependent variables were sagittal and coronal muscle angles. Independent variables were: (i) craniofacial group, (ii) sex, and (iii) muscle.

Hypothesis 4: There were no differences in the sagittal and coronal angulations of the masseter or temporalis muscles between female and male subjects. Dependent variables were sagittal and

coronal muscle angles. Independent variables were: (i) craniofacial group, (ii) sex, and (iii) muscle.

For all hypotheses, analysis of variance (ANOVA) and Tukey's honest significant difference (HSD) posthoc tests were used to compare the dependent variable for significant effects of the independent variables, where significance was defined by a p value < 0.05 (Appendices 1 – 21).

RESULTS

Subjects

Data for one-hundred forty-seven subjects were reviewed. Ninety subjects were excluded based on FHMPA of >22 and <28 degrees. Fifty-seven subjects were included in the study. Thirty-five of the subjects were female, of which nineteen were dolichofacial and sixteen were brachyfacial types. Twenty-two of the subjects were male, of which ten were dolichofacial and twelve were brachyfacial types. The mean FHMPA \pm standard deviation for dolichofacial subjects was $31.9^\circ \pm 4.5^\circ$ and for brachyfacial subjects was $18.2^\circ \pm 2.8^\circ$ (Table 1). The dolichofacial subjects' had an average age of 28.0 ± 10.3 years and the brachyfacial subjects' had an average age of 33.6 ± 12.6 years.

Refinement of the geometry files was done so that the predicted eminence shape matches the right or left measured eminence form. Geometry file refinement was needed for 18 of the 57 total subjects. The range of masseter and temporalis muscle centroid position changes were from -9mm to $+10\text{mm}$ through iterative changes of $\pm 2\text{-}3\text{mm}$ at a time until there was a match between the revised predicted and measured eminence forms. We were able to match at least the right or left measured eminence forms to the predicted or modified-predicted eminence forms for all subjects included in the study.

	Dolichofacial Group	Brachyfacial Group
Number of Females	19	16
Number of Males	10	12
Total Number	29	28
FHMPA	$31.9^{\circ} \pm 4.5^{\circ}$	$18.2^{\circ} \pm 2.8^{\circ}$
Age (years)	28.0 ± 10.3	33.6 ± 12.6

Table 1: Numbers of subjects, Frankfort horizontal mandibular plane angle (FHMPA, mean \pm standard deviation), and age (mean \pm standard deviation) for two diagnostic groups.

Three-dimensional geometry differences between diagnostic groups

In general, male dolichofacial subjects exhibited greater sagittal and coronal angulations in the masseter muscle vector (main direction of activation) relative to the occlusal plane compared to male brachyfacial subjects and these differences were nearly statistically significant for both the sagittal ($p=0.085$) and coronal ($p=0.091$) angulations. The sagittal angulations of the dolichofacial and brachyfacial male subjects' masseter muscle vectors were $63.9^{\circ} \pm 8.9^{\circ}$ and $57.7^{\circ} \pm 7.0^{\circ}$, respectively. The coronal angulations of the dolichofacial and brachyfacial male subjects' masseters were $38.8^{\circ} \pm 14.2^{\circ}$ and $30.9^{\circ} \pm 5.3^{\circ}$, respectively (Figure 7). There were no statistically significant differences in masseter muscle angulations between dolichofacial and brachyfacial females. Dolichofacial females had masseter muscle sagittal and coronal angulations of $54.2^{\circ} \pm 10.5^{\circ}$ and $27.8^{\circ} \pm 7.9^{\circ}$, respectively. Whereas, brachyfacial females had masseter muscle sagittal and coronal angulations of $55.7^{\circ} \pm 9.0^{\circ}$ and $31.9^{\circ} \pm 11.9^{\circ}$, respectively.

Within the dolichofacial group, there was a statistically significant sex difference in the three-dimensional orientation of the masseter sagittal and coronal vectors. The male dolichofacial subjects had a sagittal masseter angle of $63.9^\circ \pm 8.9^\circ$ whereas in the females this angle was $54.2^\circ \pm 10.5$ ($p=0.019$). The male dolichofacial masseter coronal angulation was $38.8^\circ \pm 14.2^\circ$, and was significantly larger ($p=0.012$) than the female dolichofacial masseter coronal angulation ($27.8^\circ \pm 7.9^\circ$, Figure 7). No statistically significant sex differences were found for masseter sagittal and coronal vectors within the brachyfacial group.

No statistically significant sex or diagnostic group differences were found for temporalis muscle geometries (Figure 8). However, there were trends with the TSA and TCA being greater for dolichofacial compared to brachyfacial males and opposite for females. The TCA angulations tended to have much larger standard deviations on average than the TSA angulations. This may be in part due to the limited field of view in the CBCT exposures, which were cut posteriorly to limit the radiation exposure to the subjects, leading to difficulties in identifying the temporalis muscle origin centroid locations accurately in the geometry files used for TCA angulation measurements.

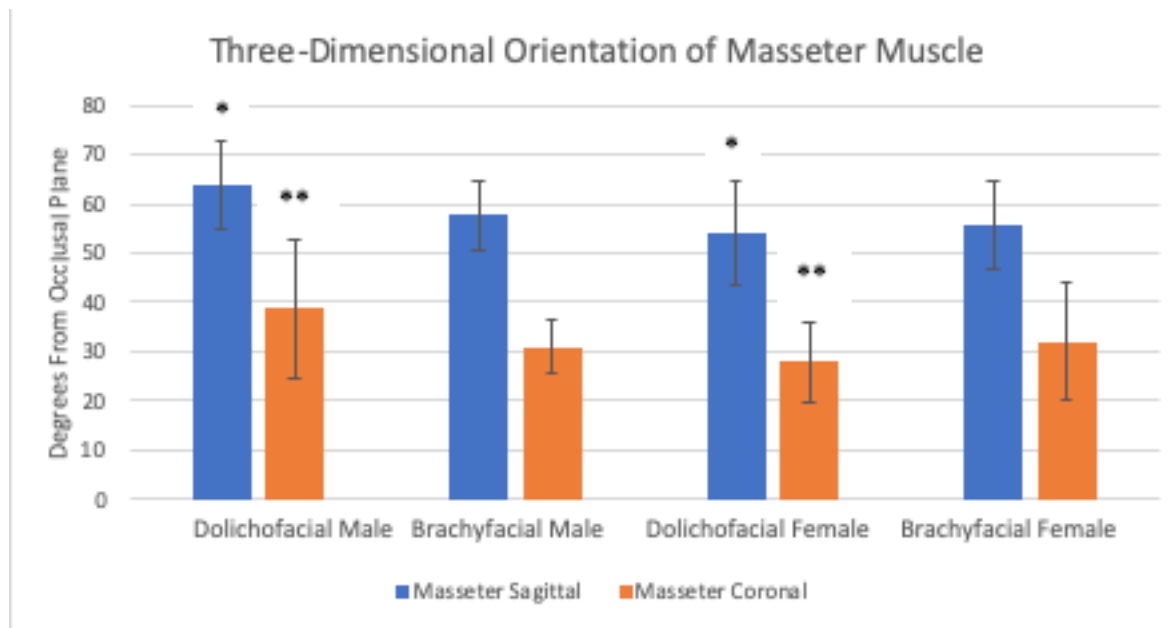


Figure 7: Sex and diagnostic group differences in masseter orientation as related to the occlusal plane. * The male dolichofacial subjects had a sagittal masseter angle of $63.9^{\circ} \pm 8.9^{\circ}$ whereas the female angle was $54.2^{\circ} \pm 10.5$ ($p=0.019$). **The male dolichofacial masseter coronal angulation was $38.8^{\circ} \pm 14.2^{\circ}$ and the female dolichofacial masseter coronal angulation was $27.8^{\circ} \pm 7.9^{\circ}$ ($p=0.012$).

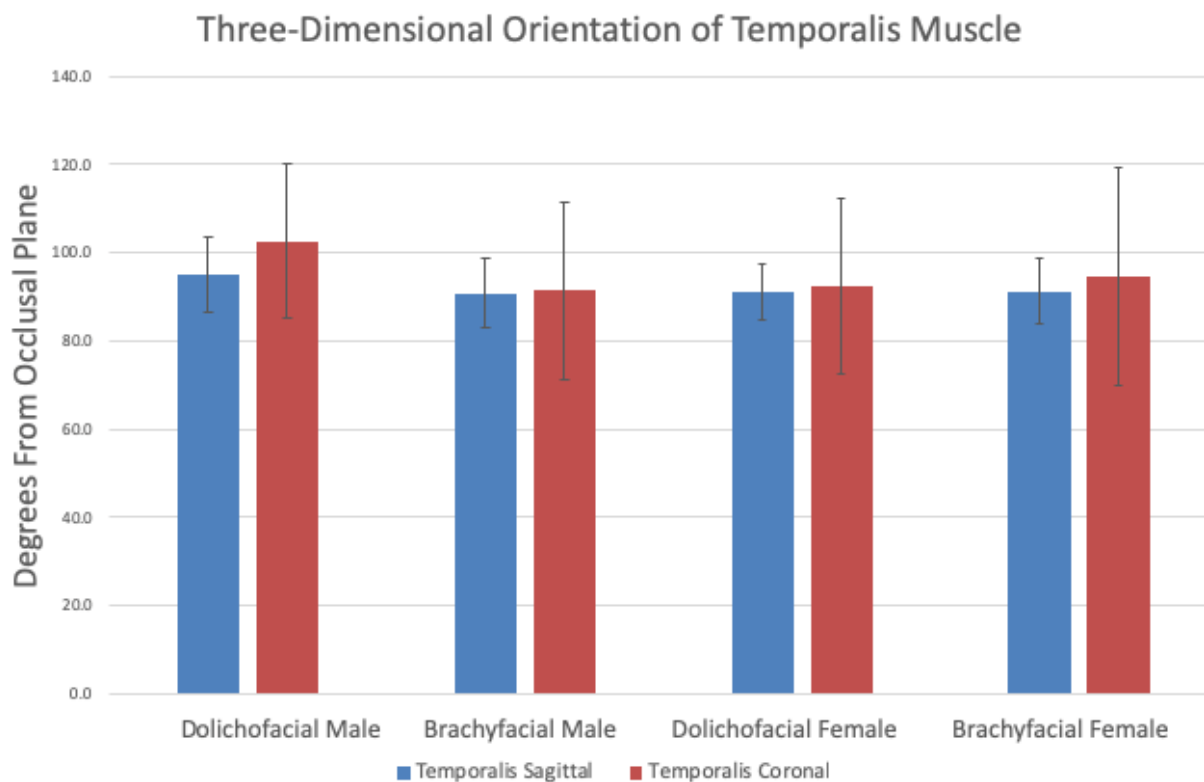


Figure 8: Sex and diagnostic group differences in temporalis orientation as related to occlusal plane. No statistically significant findings were made for the temporalis muscle geometries between sexes or diagnostic groups.

Ipsilateral TMJ loads

Ipsilateral joint loads (average, negative bite force angles, positive bite force angles) in the female brachyfacial ($80.7 \pm 22.5\%$, $77.5 \pm 25.5\%$, $83.3 \pm 22.1\%$) and dolichofacial subjects ($82.4 \pm 33.7\%$, $79.3 \pm 34.2\%$, $84.9 \pm 34.3\%$) were not statistically significantly different (Figure 9). The ipsilateral joint loads (average, negative bite force angles, positive bite force angles) in the male brachyfacial ($97.9 \pm 33.6\%$, $97.7 \pm 35.6\%$, $98.1 \pm 32.9\%$) and dolichofacial subjects ($106.4 \pm 72.3\%$, $106.7 \pm 78.7\%$, $106.2 \pm 68.6\%$) were also not statistically significantly different (Figure 10).

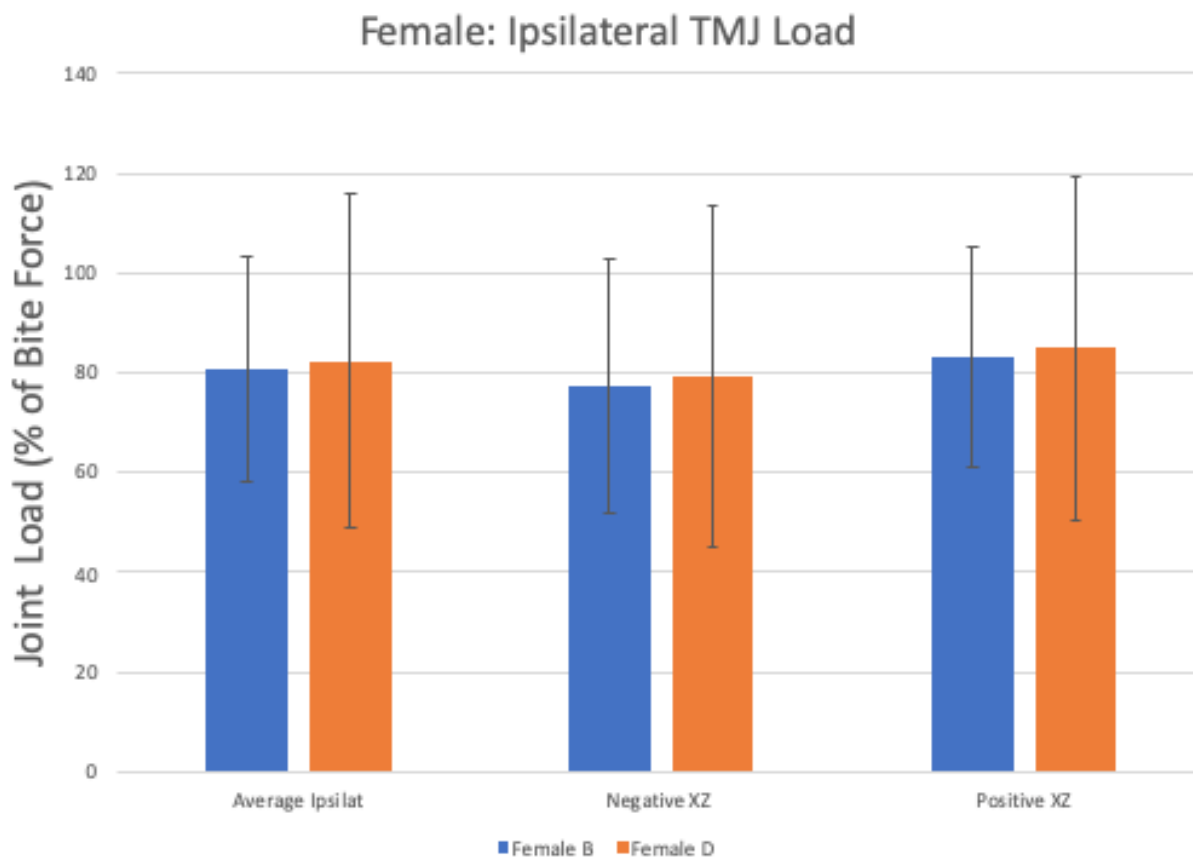


Figure 9: Diagnostic group differences in female ipsilateral temporomandibular joint (TMJ) loads. Average joint loads included all biting angles. A distolabial bite-force vector on the right mandibular canine was produced by a negative ($360\text{-}320^\circ$) series of biting angles. A distolingual bite-force vector was produced by a positive ($0\text{ to }40^\circ$) series of biting angles. TMJ loads were expressed as a percentage of a 100-unit bite force. B=brachyfacial and D=dolichofacial.

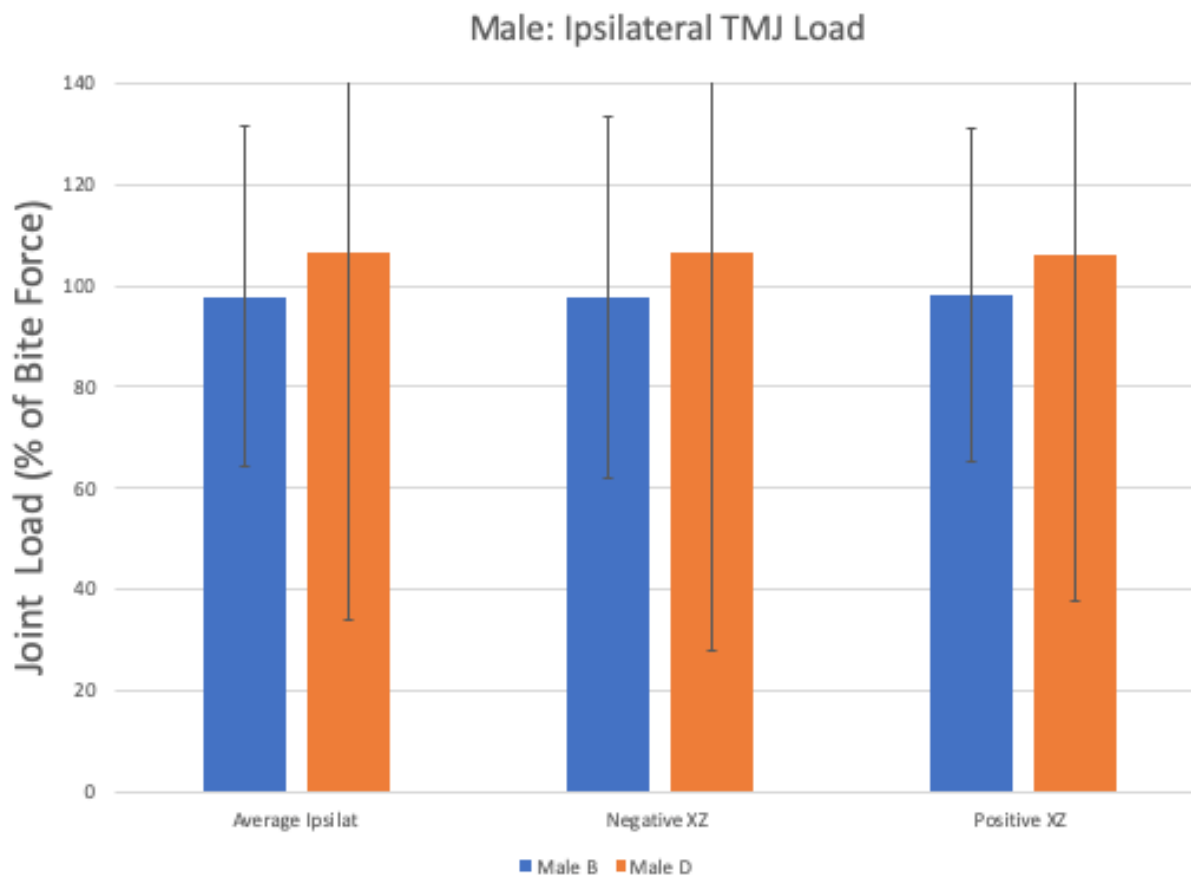


Figure 10: Diagnostic group differences in male ipsilateral temporomandibular joint (TMJ) loads. Average joint loads included all biting angles. A distolabial bite force vector on the right mandibular canine was produced by a negative (360-320°) series of biting angles. A distolingual bite-force vector was produced by a positive (0 to 40°) series of biting angles. TMJ loads were expressed as a percentage of a 100-unit bite force. B=brachyfacial and D=dolichofacial.

Contralateral TMJ loads

Contralateral joint loads (average, negative bite force angles, positive bite force angles) in female brachyfacial subjects (82.5±24.6%, 87.2±27.9%, 78.8±22.7%) were smaller than in dolichofacial subjects (95.3±27.7%, 99.5±30.1%, 92.0±26.2%). However, these differences were not statistically significant (Figure 11). Similarly, contralateral joint loads (average, negative bite

force angles, positive bite force angles) in male brachyfacial subjects ($90.8\pm 30.0\%$, $92.2\pm 34.2\%$, $89.7\pm 27.7\%$) were smaller than in dolichofacial subjects ($112.4\pm 39.2\%$, $118.0\pm 43.6\%$, $108.0\pm 36.0\%$) but these differences were not statistically significant (Figure 12).

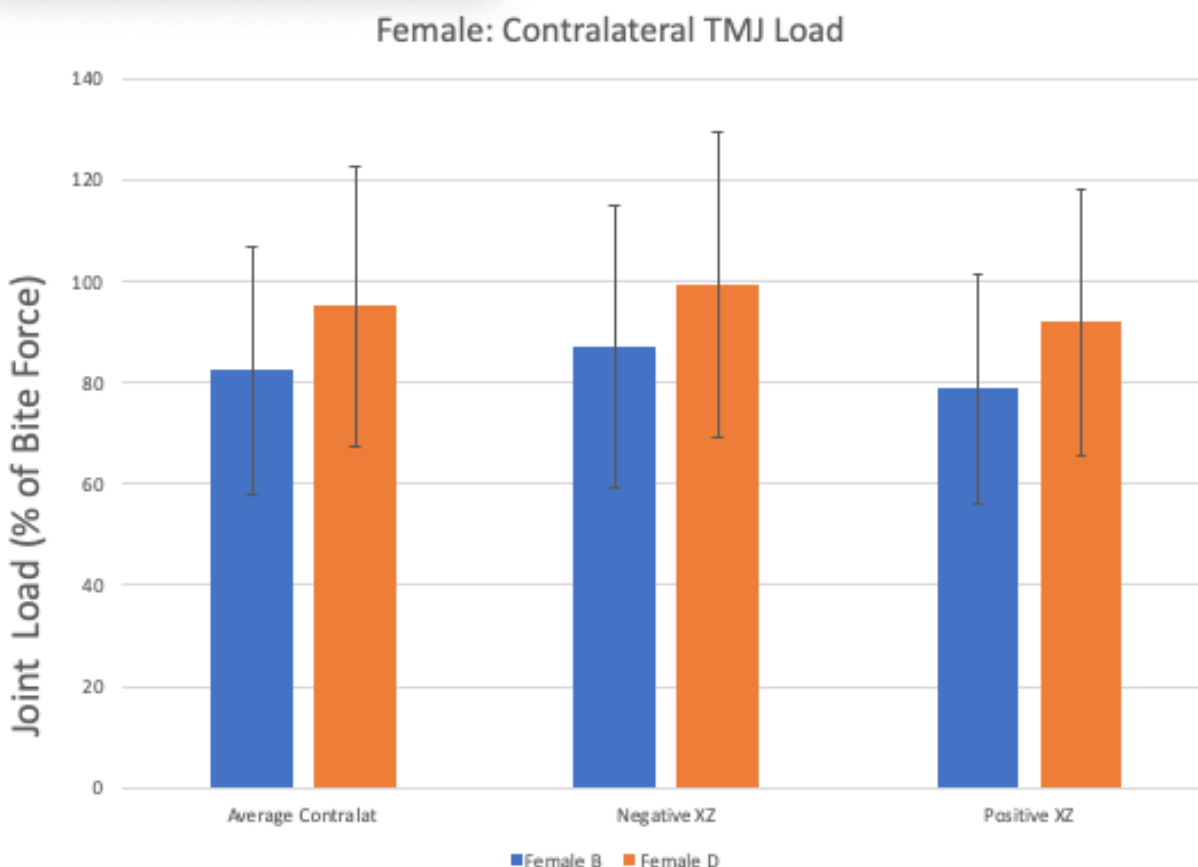


Figure 11: Diagnostic group differences in female contralateral temporomandibular joint (TMJ) loads. Average joint loads included all biting angles. A distolabial bite-force vector on the right mandibular canine was produced by a negative ($360\text{--}320^\circ$) series of biting angles. A distolingual bite-force vector was produced by a positive ($0\text{ to }40^\circ$) series of biting angles. TMJ loads were expressed as a percentage of a 100-unit bite force. B=brachyfacial and D=dolichofacial.

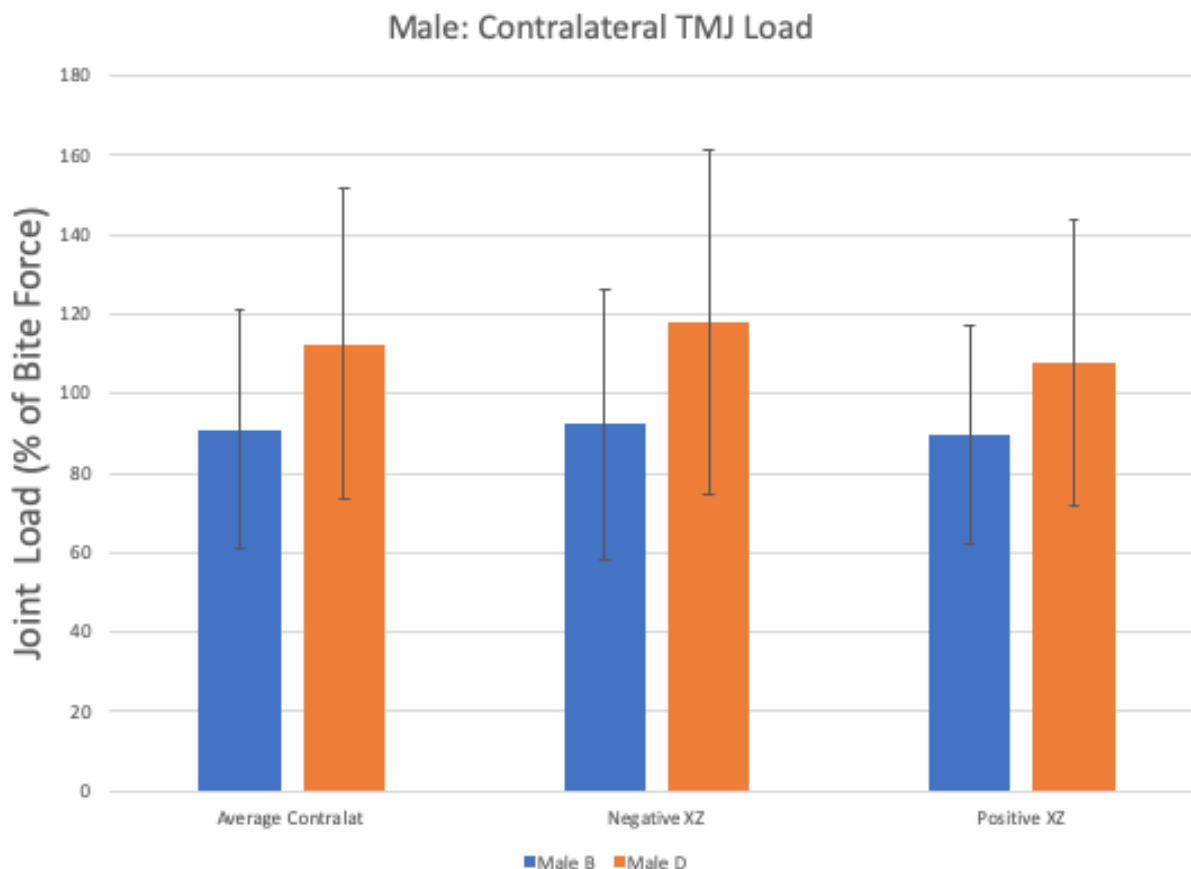


Figure 12: Diagnostic group differences in male contralateral temporomandibular joint (TMJ) loads. Average joint loads included all biting angles. A distolabial bite-force vector on the right mandibular canine was produced by a negative ($360\text{-}320^\circ$) series of biting angles. A distolingual bite-force vector was produced by a positive ($0\text{ to }40^\circ$) series of biting angles. TMJ loads were expressed as a percentage of a 100-unit bite force. B=brachyfacial and D=dolichofacial.

Sex and Diagnostic Group Differences in Overall Average TMJ Loads

Generally, males in both craniofacial groups had higher overall TMJ loads for all canine biting angles combined as compared to females in both craniofacial groups (Figure 13). When craniofacial groups were combined, overall TMJ loads for all biting angles combined in the male subjects ($101.31 \pm 5.1\%$) were 15.7% and significantly larger (Figure 14, $p < 0.01$) compared to

those in the female subjects ($85.6 \pm 28.4\%$). When sexes were combined, overall TMJ loads for all canine biting angles combined in the dolichofacial subjects $96.0 \pm 42.8\%$ were 8.9% and significantly larger (Figure 15, $p=0.018$) compared to those in the brachyfacial subjects $87.1\% \pm 28.1\%$.

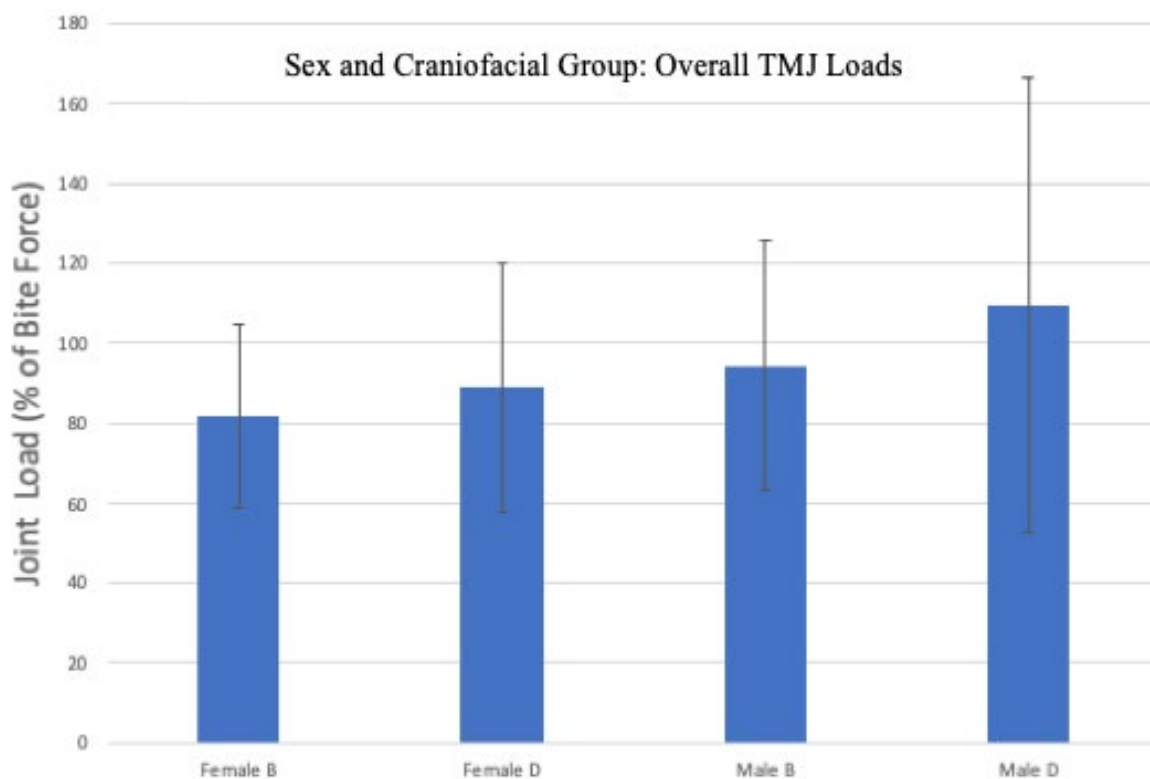


Figure 13: Sex and craniofacial group (D=dolichofacial; B=brachyfacial) differences in overall temporomandibular joint (TMJ) loads as percent of applied bite force. Ipsilateral and contralateral TMJ loads for all canine biting angles were used to produce average overall joint loads.

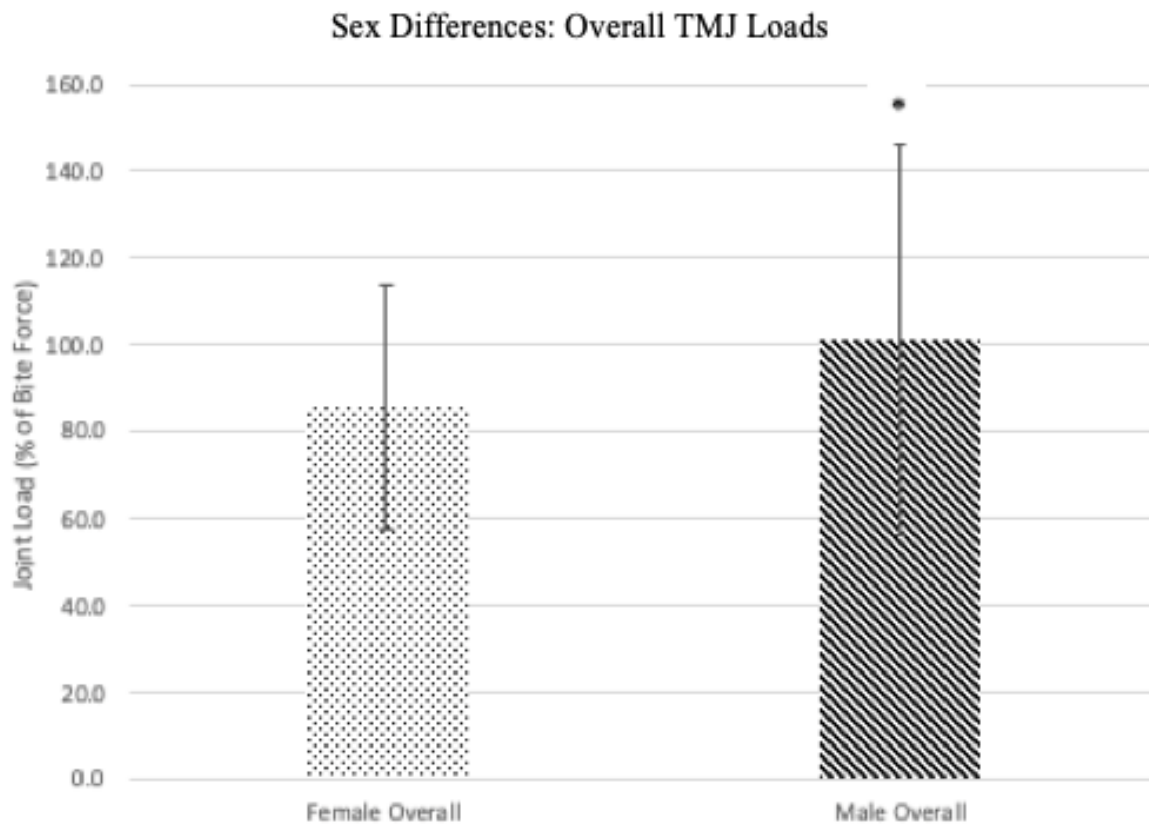


Figure 14: Sex differences in overall temporomandibular joint (TMJ) loads as percent of applied bite force. Ipsilateral and contralateral TMJ loads for all canine biting angles were used to produce average overall joint loads. * The overall joint loads of the male subjects ($101.3 \pm 5.1\%$) were significantly larger ($p < 0.01$) than those of the females (85.6 ± 28.4) by 15.7%.

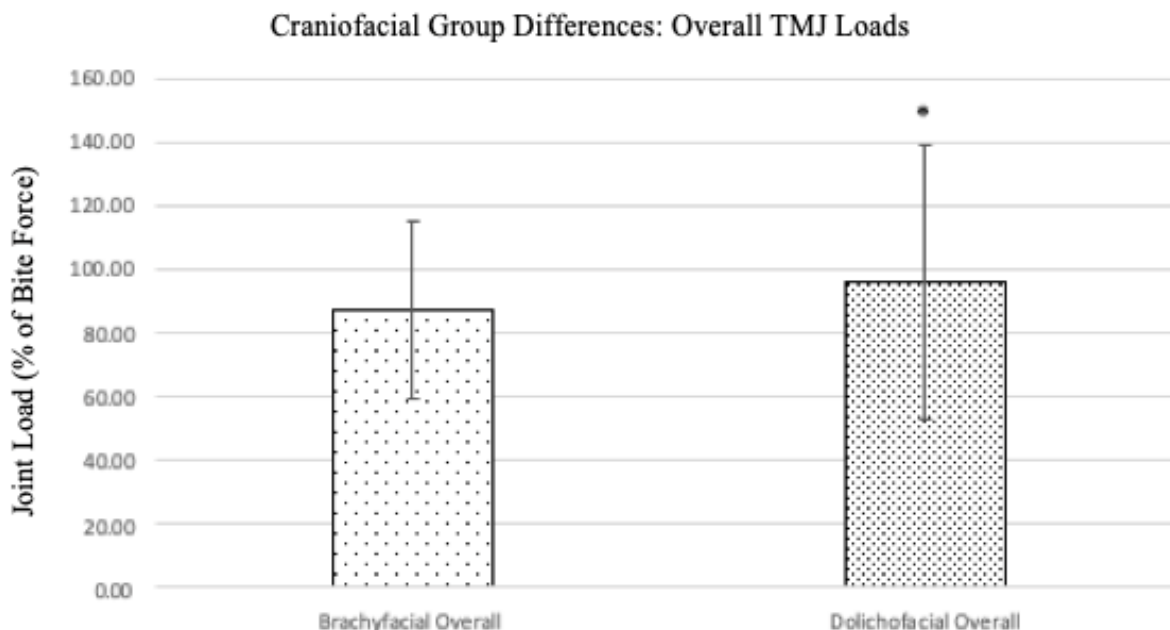


Figure 15: Craniofacial group differences in overall temporomandibular joint (TMJ) loads as percent of applied bite force. Ipsilateral and contralateral TMJ loads for all canine biting angles were used to produce average joint loads. * The overall TMJ loads of the dolichofacial group ($96.0 \pm 42.8\%$) were significantly larger ($p=0.018$) on average than the brachyfacial group ($87.1\% \pm 28.1$).

A power analysis was performed to determine how many subjects were necessary to detect significant differences in ipsilateral and contralateral TMJ loads for the independent variables of (i) sex, (ii) craniofacial group, and (iii) TMJ. Two different indices were used, where in the first calculation (Index 1) the false-negative and false-positive criteria were $\alpha = 0.05$ and $\beta = 0.80$. A second analysis (Index 2) had criteria of $\alpha = 0.05$ and $\beta = 0.85$. The results produced by the Index 1 criteria indicated that 64 brachyfacial subjects (40 female, 24 male) and 64 dolichofacial subjects (40 female, 24 male) were required to demonstrate statistically significant sex and diagnostic group differences for the ipsilateral and contralateral TMJ loads. For the

slightly more stringent Index 2 criteria, 73 brachyfacial subjects (45 female, 28 male) and 73 dolichofacial subjects (45 female, 28 male) were required to achieve power.

Gender	Computed N per Group				
	Index	Nominal Power	Actual Alpha	Actual Power	N per Group
F	1	0.8	0.05	0.801	40
	2	0.85	0.05	0.851	45
M	1	0.8	0.05	0.801	24
	2	0.85	0.05	0.852	28

Figure 16: Power analysis of data where N=number of subjects, F=female, M=male, Index 1 had criteria of $\alpha = 0.05$ and $\beta = 0.80$. Index 2 had criteria of $\alpha = 0.05$ and $\beta = 0.85$.

DISCUSSION

TMJ Loads

This study evaluated if overall, ipsilateral, and contralateral TMJ loads differed between craniofacial groups, and between adult females and males. The results demonstrated that on average the dolichofacial group had TMJ loads that were 8.9% higher than TMJ loads in brachyfacial group. The findings were consistent with previous studies comparing brachyfacial and dolichofacial groups, where dolichofacial subjects had ipsilateral joint loads that were $\geq 20\%$ for incisor biting that tended to push the jaw posteromedially ($\theta_Y=0-25^\circ$, $\theta_{XZ}=315-350^\circ$) and molar biting that tended to push the jaw posterolaterally ($\theta_Y=35-40^\circ$, $\theta_{XZ}=70-140^\circ$).² Another study showed that dolichofacial subjects had higher joint loads of $\geq 20\%$ at 12 years and 18 years of age compared to brachyfacial subjects. These differences were produced by specific biting angles for both the ipsilateral and contralateral joints.⁴⁰ The overall TMJ loads in this study were 15.7% higher in males when compared with females. A previous study reported TMJ loads in

healthy subjects that were a sub-sample of the current study and showed contralateral loads were generally higher than for ipsilateral and were not markedly different between females (16.3 ± 4.2 N) and males (15.7 ± 2.6 N). Assuming a 20 N applied canine bite force, as in the previous study, the current study showed overall TMJ loads of 17.1 ± 5.7 N for females and 20.3 ± 1.02 N for males. One explanation for the differences in sex results could be that many of the subjects in the current study had disc displacement. The same previous study also calculated mean energy densities (\pm standard deviations), the concentration of mechanical work done in ipsilateral and contralateral TMJs during jaw closing from an open position, and found that in females these were 9.0 ± 9.7 and 8.4 ± 5.5 mJ/mm³, respectively, and were significantly larger compared to ipsilateral and contralateral TMJs in males, which were 5.6 ± 4.2 and 6.3 ± 4.2 mJ/mm³, respectively.²⁸ One of the limitations of the current study was that there was no consideration of the compressive stresses or energy densities in the ipsilateral and contralateral TMJs. Future investigations should investigate the differences in condyle and articular disc size in an evaluation of sex differences in compressive stresses and energy densities. For example, although men tend to have larger joint loads, they also have larger condyles over which the loads are distributed, thereby creating compressive stresses which may be significantly lower compared to females. Additionally, sex and diagnostic group differences in congruency of the bony surfaces of the TMJ influences the distribution of loads. Future research should explore if there are sex and diagnostic group differences in TMJ eminence slopes since steepness of the TMJ eminence slope has been correlated with reduced congruency of the TMJ loading surfaces and increased stress concentration.²⁹ Previously mentioned studies have shown that healthy females have TMJ energy densities that are significantly larger than in males. The higher energy densities may predispose females to earlier mechanical fatigue of the TMJ disc. Future studies

should evaluate sex and craniofacial group as well as temporomandibular disorder diagnostic group differences in TMJ energy densities. Energy density is related to TMJ loads, which were the focus of the current study, but also takes into account size of condyle and articular disc tissues over which the forces are distributed.

Validation of Model-predicted TMJ Sagittal Effective Eminence Shape

Through a validation process we were able to refine the geometry files and validate the eminence predictor modeling program. Using the eminence comparison program, we were able to confirm matches between the right or left measured eminence forms and the predicted eminence forms. The eminence creator program was quite accurate in its predictions of the true or measured eminence forms. Of the 18 subjects that needed modifications of their geometry files due to inaccurate eminence predictions the range of masseter muscle orientation changes were -9mm to 10mm. Majority of the iterative changes that were made in the geometry files were less than 3-4mm. All 14 subject's geometry files were able to be modified so that a match was obtained between the two eminence forms. This validation will allow for more accurate model predictions and accurate results in future research using the eminence creator program.

Three-Dimensional Muscle Geometries

This study tested if brachyfacial and dolichofacial groups, or sexes, differed in three-dimensional muscle geometries, with a primary focus on the sagittal and coronal angulations of the masseter and temporalis muscles. The results for three-dimensional masseter muscle geometries showed near significant differences between dolichofacial and brachyfacial male subjects. There were significant differences in masseter muscle coronal and sagittal angulations between males and females within the dolichofacial group. A previous study⁴¹ which used three-

dimensional computed tomography imaging of children showed diagnostic group differences in orientation of the medial pterygoid and masseter muscles. They showed that in subjects with a dolichofacial phenotype, the line of action of the medial pterygoid muscle and anterior border of the masseter seem to be more acute relative to the Frankfort horizontal plane (FHP) compared to brachyfacial individuals. Similar findings from other studies reported that the angulation of the masseter becomes more acute relative to FHP and sella-nasion plane as the mandibular plane becomes steeper.^{42 43} Although our study didn't provide craniofacial type differences in muscle orientation there were near statistically significant differences. This may have been in part due to the differences in measures of the muscle orientation, where in our study we used muscle centroids and the previous studies mentioned looked at the anterior border of the masseter muscle. We also used a functional plane, occlusal plane, as our reference line whereas previous studies have looked at muscle orientation with respect to FHP. The results of these studies in combination with the current results suggested that the angular orientations of the muscles of mastication might influence the craniofacial skeletal morphology, and in particular TMJ loads between dolichofacial and brachyfacial phenotypes. The variation in muscle orientations and TMJ loads may alter the vertical and horizontal growth patterns within the mandible by stimulating or inhibiting the cells in the condylar growth region. Future research is needed to do a longitudinal CBCT imaging project to evaluate how the muscles of mastication change and adapt with growth and development of the craniofacial complex.

Limitations

A single cephalometric image is not as useful as longitudinal imaging to evaluate growth changes in an individual over time. In future research it may be of importance to identify subjects with brachyfacial and dolichofacial phenotypes early in life and follow them using

longitudinal three-dimensional imaging techniques to evaluate changes in the dentofacial skeleton, orientation changes in the muscles of mastication, and TMJ loads. It should be noted that the subjects in this study were of adult age and growth had subsided. The data produced from this study require testing by comparing with data measured from growing subjects.

The current study focused primarily on static biting-forces on the canine, with a limited range of vectors which directed the mandible posteriorly, posteromedially and posterolaterally. Additionally, the study did not include biting angulations at other positions such as at the incisors or molars. A more complete investigation should be done which involves more biting locations and angles. Additionally, future research should attempt to quantify true loading behaviors or how individuals actually bite on any given teeth and at what range of angles.

To enhance future investigations, it should be noted that a limitation of the current study was the assumption of right-left symmetry of the muscles of mastication. As well, it was common to find asymmetry between the right and left *in vivo* measured eminence shapes. The modeling methodology used in the current study was limited in that an acceptable geometry file was determined based on the ability of the numerical model to predict a shape that matched either right or left measured morphology. Given that it was common to have asymmetries between the right and left eminence forms, model calculated TMJ loads may be different from *in vivo* loads on the right versus the left.

CONCLUSIONS

Diagnostic group and sex differences in TMJ load

Hypothesis 1: There were no differences in ipsilateral, contralateral, and overall TMJ loads between brachyfacial and dolichofacial individuals

- f) Dolichofacial subjects had significantly higher average TMJ loads than brachyfacial subjects.
- g) Between diagnostic groups, there were no sex differences in TMJ loads.

Hypothesis 2: There were no sex differences in ipsilateral, contralateral, and overall TMJ loads during static canine biting conditions.

- h) Male subjects had significantly higher average joint loads compared to females.
- i) Within diagnostic groups, although males had higher ipsilateral and contralateral TMJ loads compared to females, differences were not statistically significant.
- j) Within diagnostic groups, although males had higher ipsilateral and contralateral TMJ loads compared to females, differences were not statistically significant.

Diagnostic Group and Sex Differences in Muscle Geometry

Hypothesis 3: There were no differences in the sagittal and coronal angulations of the masseter or temporalis muscles between brachyfacial and dolichofacial groups.

- f) Dolichofacial males exhibited larger, and near statistically significant, sagittal and coronal angulations compared to brachyfacial males.
- g) There were no statistically significant differences in muscle geometries between dolichofacial and brachyfacial women.

Hypothesis 4: There were no differences in the sagittal and coronal angulations of the masseter or temporalis muscles between female and male subjects.

- h) There were statistically significant difference in masseter muscle geometry between dolichofacial men and women.
- i) No statistically significant differences were found in masseter angulations between brachyfacial men and women.
- j) No statistically significant sex or diagnostic group differences were found for temporalis muscle geometry.

REFERENCES

1. Franco FC, de Araujo TM, Vogel CJ, Quintao CC. Brachycephalic, dolichocephalic and mesocephalic: Is it appropriate to describe the face using skull patterns? *Dental Press J Orthod* 2013;18:159-163.
2. Nickel JC, Weber AL, Covington Riddle P, Liu Y, Liu H, Iwasaki LR. Mechanobehaviour in dolichofacial and brachyfacial adolescents. *Orthod Craniofac Res* 2017;20 Suppl 1:139-144.
3. Nanda SK. Patterns of vertical growth in the face. *Am J Orthod Dentofacial Orthop* 1988;93:103-116.
4. Iwasaki LR, Baird BW, McCall WD, Jr., Nickel JC. Muscle and temporomandibular joint forces associated with chincup loading predicted by numerical modeling. *Am J Orthod Dentofacial Orthop* 2003;124:530-540.
5. Iwasaki LR, Crosby MJ, Marx DB, Gonzalez Y, McCall WD, Jr., Ohrbach R et al. Human temporomandibular joint eminence shape and load minimization. *J Dent Res* 2010;89:722-727.
6. Bjork A, Skieller V. Facial development and tooth eruption. An implant study at the age of puberty. *Am J Orthod* 1972;62:339-383.
7. Nahhas RW, Valiathan M, Sherwood RJ. Variation in timing, duration, intensity, and direction of adolescent growth in the mandible, maxilla, and cranial base: the Fels longitudinal study. *Anat Rec (Hoboken)* 2014;297:1195-1207.
8. Ackerman JL, Proffit WR. Communication in orthodontic treatment planning: bioethical and informed consent issues. *Angle Orthod* 1995;65:253-261.
9. Sassouni V. A classification of skeletal facial types. *Am J Orthod* 1969;55:109-123.
10. Ricketts RM. The Influence Of Orthodontic Treatment On Facial Growth And Development. *The Angle Orthodontist* 1960;30:103-133.
11. Fields HW, Proffit WR, Nixon WL, Phillips C, Stanek E. Facial pattern differences in long-faced children and adults. *Am J Orthod* 1984;85:217-223.
12. Bishara SE, Augspurger EF, Jr. The role of mandibular plane inclination in orthodontic diagnosis. *Angle Orthod* 1975;45:273-281.
13. ISAACSON JR, ISAACSON RJ, SPEIDEL TM, WORMS FW. Extreme Variation in Vertical Facial Growth and Associated Variation in Skeletal and Dental Relations. *The Angle Orthodontist* 1971;41:219-229.
14. Bishara SE, Jakobsen JR. Longitudinal changes in three normal facial types. *Am J Orthod* 1985;88:466-502.
15. Siritwat PP, Jarabak JR. Malocclusion and facial morphology is there a relationship? An epidemiologic study. *Angle Orthod* 1985;55:127-138.
16. Schudy FF. Vertical Growth Versus Anteroposterior Growth As Related To Function And Treatment. *The Angle Orthodontist* 1964;34:75-93.
17. Itaru Mizoguchi NT, Yuya Nakao. Growth of the mandible and biological characteristics of the mandibular condylar cartilage. *Japanese Dental Science Review* 2013:139-150.
18. Copray JC, Jansen HW, Duterloo HS. Effects of compressive forces on proliferation and matrix synthesis in mandibular condylar cartilage of the rat in vitro. *Arch Oral Biol* 1985;30:299-304.

19. Karlo CA, Stolzmann P, Habernig S, Muller L, Saurenmann T, Kellenberger CJ. Size, shape and age-related changes of the mandibular condyle during childhood. *Eur Radiol* 2010;20:2512-2517.
20. Knothe Tate ML, Falls TD, McBride SH, Atit R, Knothe UR. Mechanical modulation of osteochondroprogenitor cell fate. *Int J Biochem Cell Biol* 2008;40:2720-2738.
21. Nickel JC, Iwasaki LR, Gonzalez YM, Gallo LM, Yao H. Mechanobehavior and Ontogenesis of the Temporomandibular Joint. *J Dent Res* 2018;97:1185-1192.
22. Copray JC, Jansen HW, Duterloo HS. Growth and growth pressure of mandibular condylar and some primary cartilages of the rat in vitro. *Am J Orthod Dentofacial Orthop* 1986;90:19-28.
23. Hichijo N, Kawai N, Mori H, Sano R, Ohnuki Y, Okumura S et al. Effects of the masticatory demand on the rat mandibular development. *J Oral Rehabil* 2014;41:581-587.
24. Batista KB, Thiruvenkatachari B, Harrison JE, O'Brien KD. Orthodontic treatment for prominent upper front teeth (Class II malocclusion) in children and adolescents. *Cochrane Database Syst Rev* 2018;3:Cd003452.
25. Baume LJ, Derichsweiler H. Is the condylar growth center responsive to orthodontic therapy? An experimental study in *Macaca mulatta*. *Oral Surg Oral Med Oral Pathol* 1961;14:347-362.
26. Martins LF, Vigorito JW. Photometric analysis applied in determining facial type. *Dental Press Journal of Orthodontics* 2012;17:71-75.
27. Edwards CB, Marshall SD, Qian F, Southard KA, Franciscus RG, Southard TE. Longitudinal study of facial skeletal growth completion in 3 dimensions. *Am J Orthod Dentofacial Orthop* 2007;132:762-768.
28. Iwasaki LR, Gonzalez YM, Liu Y, Liu H, Markova M, Gallo LM et al. TMJ energy densities in healthy men and women. *Osteoarthritis Cartilage* 2017;25:846-849.
29. Nickel JC, Iwasaki LR, Gallo LM, Palla S, Marx DB. Tractional Forces, Work and Energy Densities in the Human TMJ. *Craniofac Growth Ser* 2009;46:427-450.
30. Nickel JC, Iwasaki LR, Walker RD, McLachlan KR, McCall WD, Jr. Human masticatory muscle forces during static biting. *J Dent Res* 2003;82:212-217.
31. Nickel JC, Yao P, Spalding PM, Iwasaki LR. Validated numerical modeling of the effects of combined orthodontic and orthognathic surgical treatment on TMJ loads and muscle forces. *Am J Orthod Dentofacial Orthop* 2002;121:73-83.
32. Gallo LM, Nickel JC, Iwasaki LR, Palla S. Stress-field translation in the healthy human temporomandibular joint. *J Dent Res* 2000;79:1740-1746.
33. Faulkner MG, Hatcher DC, Hay A. A three-dimensional investigation of temporomandibular joint loading. *J Biomech* 1987;20:997-1002.
34. Koriotoh TW, Hannam AG. Effect of bilateral asymmetric tooth clenching on load distribution at the mandibular condyles. *J Prosthet Dent* 1990;64:62-73.
35. Trainor PG, McLachlan KR, McCall WD. Modelling of forces in the human masticatory system with optimization of the angulations of the joint loads. *J Biomech* 1995;28:829-843.
36. Nickel JC, Gonzalez YM, McCall WD, Ohrbach R, Marx DB, Liu H et al. Muscle organization in individuals with and without pain and joint dysfunction. *J Dent Res* 2012;91:568-573.
37. Ahmad M, Hollender L, Anderson Q, Kartha K, Ohrbach R, Truelove EL et al. Research diagnostic criteria for temporomandibular disorders (RDC/TMD): development of image

analysis criteria and examiner reliability for image analysis. *Oral Surg Oral Med Oral Pathol Oral Radiol Endod* 2009;107:844-860.

38. Gallo LM, Fankhauser N, Gonzalez YM, Liu H, Liu Y, Nickel JC et al. Jaw closing movement and sex differences in temporomandibular joint energy densities. *J Oral Rehabil* 2018;45:97-103.

39. Schiffman E, Ohrbach R, Truelove E, Look J, Anderson G, Goulet JP et al. Diagnostic Criteria for Temporomandibular Disorders (DC/TMD) for Clinical and Research Applications: recommendations of the International RDC/TMD Consortium Network* and Orofacial Pain Special Interest Groupdagger. *J Oral Facial Pain Headache* 2014;28:6-27.

40. Iwasaki LR, Liu Y, Liu H, Nickel JC. Jaw mechanics in dolichofacial and brachyfacial phenotypes: A longitudinal cephalometric-based study. *Orthod Craniofac Res* 2017;20 Suppl 1:145-150.

41. Chan HJ, Woods M, Stella D. Mandibular muscle morphology in children with different vertical facial patterns: A 3-dimensional computed tomography study. *Am J Orthod Dentofacial Orthop* 2008;133:10.e11-13.

42. Haskell B, Day M, Tetz J. Computer-aided modeling in the assessment of the biomechanical determinants of diverse skeletal patterns. *Am J Orthod* 1986;89:363-382.

43. Proctor AD, DeVincenzo JP. Masseter muscle position relative to dentofacial form. *Angle Orthod* 1970;40:37-44.

APPENDIX

Muscle Geometry Data

Appendix 1: Between-Subjects Factors Sample Size (Hypothesis 3/4).

Between-Subjects Factors		
		N
Dx Group	B	28
	D	29
Sex	F	35
	M	22

Appendix 2: descriptive statistics by diagnostic group (Hypothesis 3)

Descriptive Statistics					
Dx Group			Mean	Std. Deviation	N
MmaxSag	B	F	55.7370	9.00153	16
		M	57.7285	7.03117	12
		Total	56.5905	8.13410	28
	D	F	54.2153	10.45874	19
		M	63.8826	8.88205	10
		Total	57.5488	10.84181	29
	Total	F	54.9109	9.70818	35
		M	60.5258	8.33926	22
		Total	57.0781	9.53448	57
MmaxCoronal	B	F	31.9254	11.89179	16
		M	30.9230	5.26023	12
		Total	31.4958	9.49167	28
	D	F	27.8266	7.89354	19
		M	38.7478	14.17782	10
		Total	31.5925	11.51409	29
	Total	F	29.7004	9.98335	35
		M	34.4797	10.79558	22
		Total	31.5450	10.47505	57
TempSag	B	F	-1.2227	7.40688	16
		M	-0.8116	7.84776	12
		Total	-1.0465	7.45740	28
	D	F	-1.1396	6.16407	19
		M	-5.1839	8.50321	10
		Total	-2.5342	7.17592	29
	Total	F	-1.1776	6.65739	35
		M	-2.7990	8.25913	22
		Total	-1.8034	7.28857	57
TempCoronal	B	F	-4.5782	24.70770	16
		M	-1.3557	20.15980	12
		Total	-3.1971	22.52477	28
	D	F	-2.3171	19.97556	19
		M	-12.4665	17.50271	10
		Total	-5.8169	19.47014	29
	Total	F	-3.3508	21.95173	35
		M	-6.4061	19.39694	22
		Total	-4.5300	20.87849	57

Appendix 3: Multivariate Tests (Hypothesis 3/4)

Multivariate Tests ^a									
Effect		Value	F	Hypothesis df	Error df	Sig.	Partial Eta Squared	Noncent. Parameter	Observed Power ^c
Intercept	Pillai's Trace	0.982	664.693 ^b	4.000	50.000	0.000	0.982	2658.771	1.000
	Wilks' Lambda	0.018	664.693 ^b	4.000	50.000	0.000	0.982	2658.771	1.000
	Hotelling's Trace	53.175	664.693 ^b	4.000	50.000	0.000	0.982	2658.771	1.000
	Roy's Largest Root	53.175	664.693 ^b	4.000	50.000	0.000	0.982	2658.771	1.000
DxGroup	Pillai's Trace	0.044	.576 ^b	4.000	50.000	0.682	0.044	2.302	0.178
	Wilks' Lambda	0.956	.576 ^b	4.000	50.000	0.682	0.044	2.302	0.178
	Hotelling's Trace	0.046	.576 ^b	4.000	50.000	0.682	0.044	2.302	0.178
	Roy's Largest Root	0.046	.576 ^b	4.000	50.000	0.682	0.044	2.302	0.178
Sex	Pillai's Trace	0.105	1.474 ^b	4.000	50.000	0.224	0.105	5.895	0.424
	Wilks' Lambda	0.895	1.474 ^b	4.000	50.000	0.224	0.105	5.895	0.424
	Hotelling's Trace	0.118	1.474 ^b	4.000	50.000	0.224	0.105	5.895	0.424
	Roy's Largest Root	0.118	1.474 ^b	4.000	50.000	0.224	0.105	5.895	0.424
DxGroup * Sex	Pillai's Trace	0.088	1.201 ^b	4.000	50.000	0.322	0.088	4.803	0.349
	Wilks' Lambda	0.912	1.201 ^b	4.000	50.000	0.322	0.088	4.803	0.349
	Hotelling's Trace	0.096	1.201 ^b	4.000	50.000	0.322	0.088	4.803	0.349
	Roy's Largest Root	0.096	1.201 ^b	4.000	50.000	0.322	0.088	4.803	0.349

a. Design: Intercept + DxGroup + Sex + DxGroup * Sex

b. Exact statistic

c. Computed using alpha = .05

Appendix 4: Multivariate analysis of variance for between subject effects (Hypothesis 3/4)

Tests of Between-Subjects Effects									
Source		Type III Sum of Squares	df	Mean Square	F	Sig.	Partial Eta Squared	Noncent. Parameter	Observed Power ^a
Corrected Model	MassSag	652.581 ^a	3	217.527	2.598	0.062	0.128	7.793	0.606
	MassCoronal	788.464 ^b	3	262.821	2.601	0.062	0.128	7.802	0.606
	TempSag	139.850 ^c	3	46.617	0.871	0.462	0.047	2.614	0.227
	TempCoronal	843.878 ^d	3	281.293	0.633	0.597	0.035	1.898	0.174
Intercept	MassSag	179657.808	1	179657.808	2145.446	0.000	0.976	2145.446	1.000
	MassCoronal	56121.365	1	56121.365	555.322	0.000	0.913	555.322	1.000
	TempSag	234.038	1	234.038	4.375	0.041	0.076	4.375	0.537
	TempCoronal	1438.083	1	1438.083	3.234	0.078	0.058	3.234	0.423
DeGroup	MassSag	71.899	1	71.899	0.859	0.358	0.016	0.859	0.149
	MassCoronal	46.515	1	46.515	0.460	0.500	0.009	0.460	0.102
	TempSag	61.641	1	61.641	1.152	0.288	0.021	1.152	0.184
	TempCoronal	262.403	1	262.403	0.590	0.446	0.011	0.590	0.117
Sex	MassSag	455.421	1	455.421	5.439	0.024	0.093	5.439	0.629
	MassCoronal	329.623	1	329.623	3.262	0.077	0.058	3.262	0.426
	TempSag	44.226	1	44.226	0.827	0.367	0.015	0.827	0.145
	TempCoronal	160.763	1	160.763	0.362	0.550	0.007	0.362	0.091
DeGroup * Sex	MassSag	197.403	1	197.403	2.357	0.131	0.043	2.357	0.326
	MassCoronal	476.350	1	476.350	4.713	0.034	0.082	4.713	0.568
	TempSag	66.510	1	66.510	1.243	0.270	0.023	1.243	0.195
	TempCoronal	599.094	1	599.094	1.347	0.251	0.025	1.347	0.207
Error	MassSag	4438.174	53	83.739					
	MassCoronal	5356.228	53	101.061					
	TempSag	2835.052	53	53.492					
	TempCoronal	23567.166	53	444.664					
Total	MassSag	190791.292	57						
	MassCoronal	62864.707	57						
	TempSag	3160.279	57						
	TempCoronal	25580.738	57						
Corrected Total	MassSag	5090.756	56						
	MassCoronal	6144.692	56						
	TempSag	2974.903	56						
	TempCoronal	24411.044	56						

a. R Squared = .128 (Adjusted R Squared = .079)
b. R Squared = .128 (Adjusted R Squared = .079)
c. R Squared = .047 (Adjusted R Squared = -.007)
d. R Squared = .035 (Adjusted R Squared = -.020)
e. Computed using alpha = .05

Appendix 5: T-test group statistics of females (Hypothesis 3)

T-Test					
Sex = F					
Group Statistics ^a					
Dx Group		N	Mean	Std. Deviation	Std. Error Mean
MassSag	B	16	55.7370	9.00153	2.25038
	D	19	54.2153	10.45874	2.39940
MassCoronal	B	16	31.9254	11.89179	2.97295
	D	19	27.8266	7.89354	1.81090
TempSag	B	16	-1.2227	7.40688	1.85172
	D	19	-1.1396	6.16407	1.41413
TempCoronal	B	16	-4.5782	24.70770	6.17692
	D	19	-2.3171	19.97556	4.58271

a. Sex = F

Appendix 6: Independent samples test for females (Hypothesis 4)

		Independent Samples Test ^a										
		Levene's Test for Equality of Variances		t-test for Equality of Means							95% Confidence Interval of the Difference	
		F	Sig.	t	df	Sig. (2-tailed)	Mean Difference	Std. Error Difference	Lower	Upper		
MassSag	Equal variances assumed	0.200	0.658	0.457	33	0.651	1.52169	3.33312	-5.25959	8.30297		
	Equal variances not assumed			0.463	32.976	0.647	1.52169	3.28958	-5.17120	8.21458		
MassCoronal	Equal variances assumed	1.753	0.195	1.219	33	0.232	4.09883	3.36355	-2.74437	10.94202		
	Equal variances not assumed			1.177	25.294	0.250	4.09883	3.48106	-3.06633	11.26398		
TempSag	Equal variances assumed	1.452	0.237	-0.036	33	0.971	-0.08308	2.29285	-4.74792	4.58175		
	Equal variances not assumed			-0.036	29.295	0.972	-0.08308	2.32994	-4.84627	4.68011		
TempCoronal	Equal variances assumed	2.358	0.134	-0.299	33	0.766	-2.26109	7.55021	-17.62211	13.09993		
	Equal variances not assumed			-0.294	28.789	0.771	-2.26109	7.69127	-17.99651	13.47433		

a. Sex = F

Appendix 7: T-test group statistics for males (Hypothesis 3)

T Test						
Sex = M						
Group Statistics^a						
Dx Group		N	Mean	Std. Deviation	Std. Error Mean	
MassSag	B	12	57.7285	7.03117	2.02972	
	D	10	63.8826	8.88205	2.80875	
MassCoronal	B	12	30.9230	5.26023	1.51850	
	D	10	38.7478	14.17782	4.48342	
TempSag	B	12	-0.8116	7.84776	2.26545	
	D	10	-5.1839	8.50321	2.68895	
TempCoronal	B	12	-1.3557	20.15980	5.81963	
	D	10	-12.4665	17.50271	5.53484	

a. Sex = M

Appendix 8: Independent samples test for males (Hypothesis 4)

		Independent Samples Test^a								
		Levene's Test for Equality of Variances		t-test for Equality of Means						
		F	Sig.	t	df	Sig. (2-tailed)	Mean Difference	Std. Error Difference	95% Confidence Interval of the Difference	
									Lower	Upper
MassSag	Equal variances assumed	0.003	0.959	-1.815	20	0.085	-6.15412	3.39019	-13.22594	0.91770
	Equal variances not assumed			-1.776	17.050	0.094	-6.15412	3.46538	-13.46380	1.15556
MassCoronal	Equal variances assumed	3.514	0.076	-1.778	20	0.091	-7.82484	4.40153	-17.00626	1.35658
	Equal variances not assumed			-1.653	11.064	0.126	-7.82484	4.73359	-18.23604	2.58636
TempSag	Equal variances assumed	0.019	0.891	1.253	20	0.225	4.37234	3.48929	-2.90621	11.65088
	Equal variances not assumed			1.244	18.631	0.229	4.37234	3.51607	-2.99676	11.74143
TempCoronal	Equal variances assumed	0.408	0.530	1.365	20	0.187	11.11084	8.13965	-5.86817	28.08985
	Equal variances not assumed			1.383	19.950	0.182	11.11084	8.03135	-5.64497	27.86665

a. Sex = M

Appendix 9: T-test group statistics of brachyfacial subjects (Hypothesis 4)

T-Test					
Dx Group = B					
Group Statistics^a					
Sex		N	Mean	Std. Deviation	Std. Error Mean
MassSag	M	12	57.7285	7.03117	2.02972
	F	16	55.7370	9.00153	2.25038
MassCoronal	M	12	30.9230	5.26023	1.51850
	F	16	31.9254	11.89179	2.97295
TempSag	M	12	-0.8116	7.84776	2.26545
	F	16	-1.2227	7.40688	1.85172
TempCoronal	M	12	-1.3557	20.15980	5.81963
	F	16	-4.5782	24.70770	6.17692

a. Dx Group = B

Appendix 10: Independent samples test for brachyfacial (Hypothesis 3)

		Independent Samples Test^a											
		Levene's Test for Equality of Variances		t-test for Equality of Means								95% Confidence Interval of the Difference	
		F	Sig.	t	df	Sig. (2-tailed)	Mean Difference	Std. Error Difference	Lower		Upper		
MassSag	Equal variances assumed	2.460	0.129	0.634	26	0.532	1.99149	3.14125	-4.46544		8.44841		
	Equal variances not assumed			0.657	25.931	0.517	1.99149	3.03051	-4.23863		8.22160		
MassCoronal	Equal variances assumed	5.159	0.032	-0.272	26	0.788	-1.00248	3.68851	-8.58431		6.57935		
	Equal variances not assumed			-0.300	21.822	0.767	-1.00248	3.33830	-7.92896		5.92400		
TempSag	Equal variances assumed	0.010	0.919	0.142	26	0.888	0.41112	2.90097	-5.55192		6.37415		
	Equal variances not assumed			0.141	23.060	0.889	0.41112	2.92594	-5.64079		6.46302		
TempCoronal	Equal variances assumed	1.013	0.323	0.369	26	0.715	3.22251	8.74283	-14.74864		21.19366		
	Equal variances not assumed			0.380	25.765	0.707	3.22251	8.48661	-14.22971		20.67473		

a. Dx Group = B

Appendix 11: T-test group statistics of dolichofacial subjects (Hypothesis 4)

Dx Group = D					
Group Statistics ^a					
Sex		N	Mean	Std. Deviation	Std. Error Mean
MassSag	M	10	63.8826	8.88205	2.80875
	F	19	54.2153	10.45874	2.39940
MassCoronal	M	10	38.7478	14.17782	4.48342
	F	19	27.8266	7.89354	1.81090
TempSag	M	10	-5.1839	8.50321	2.68895
	F	19	-1.1396	6.16407	1.41413
TempCoronal	M	10	-12.4665	17.50271	5.53484
	F	19	-2.3171	19.97556	4.58271

a. Dx Group = D

Appendix 12: Independent samples test for dolichofacial subjects (Hypothesis 3)

Independent Samples Test ^a										
		Levene's Test for Equality of Variances		t-test for Equality of Means						
		F	Sig.	t	df	Sig. (2-tailed)	Mean Difference	Std. Error Difference	95% Confidence Interval of the Difference	
									Lower	Upper
MassSag	Equal variances assumed	1.732	0.199	2.484	27	0.019	9.66729	3.89155	1.68249	17.65210
	Equal variances not assumed			2.617	21.266	0.016	9.66729	3.69408	1.99089	17.34370
MassCoronal	Equal variances assumed	1.480	0.234	2.683	27	0.012	10.92119	4.07025	2.56972	19.27266
	Equal variances not assumed			2.259	12.016	0.043	10.92119	4.83533	0.38749	21.45489
TempSag	Equal variances assumed	0.391	0.537	-1.472	27	0.152	-4.04430	2.74679	-9.68026	1.59165
	Equal variances not assumed			-1.331	14.127	0.204	-4.04430	3.03813	-10.55497	2.46636
TempCoronal	Equal variances assumed	0.021	0.886	-1.354	27	0.187	-10.14942	7.49589	-25.52971	5.23086
	Equal variances not assumed			-1.412	20.704	0.173	-10.14942	7.18580	-25.10612	4.80727

a. Dx Group = D

Appendix 13: Between-Subjects factors (Hypothesis 1 and 2)

Between-Subjects Factors		
		N
DxGrip	B	168
	D	174
Sex	F	210
	M	132
Joint	Contm	171
	Ipsilat	57
	Ipsilat	114
LoadAngle	Average	114
	Negative	114
	Positive	114

Appendix 14: Tukey Post-Hoc Tests for Load Angles (Hypothesis 1 and 2)

Post Hoc Tests		
LoadAngle		
Homogeneous Subsets		
Load		
Tukey B _{ab}		
		Subset
LoadAngle	N	1
Positive	114	90.7845
Average	114	91.5911
Negative	114	92.5993
Means for groups in homogeneous subsets are displayed. Based on observed means. The error term is Mean Square(Error) = 1307.033.		
a. Uses Harmonic Mean Sample Size = 114.000.		
b. Alpha = .05.		

Appendix 15: Joint load statistics for brachyfacial subjects (Hypothesis 1)

		Descriptive Statistics				
Dependent Variable:	Load			Mean	Std. Deviation	N
Dx Grp						
B	F	Contra	Average	82.5139	24.64580	16
			Negative	87.1530	27.94150	16
			Positive	78.8027	22.69287	16
			Total	82.8232	24.88559	48
		Ipsilat	Average	80.7320	22.53874	16
			Total	80.7320	22.53874	16
		Ipsilat	Negative	77.5202	25.51157	16
			Positive	83.3014	22.12357	16
			Total	80.4108	23.67234	32
			Total	Average	81.6230	23.24939
			Negative	82.3366	26.77013	32
			Positive	81.0520	22.16375	32
		Total	81.6705	23.89166	96	
	M	Contra	Average	90.8238	30.01164	12
			Negative	92.2270	34.21684	12
			Positive	89.7012	27.65777	12
			Total	90.9173	29.87561	36
		Ipsilat	Average	97.9134	33.63109	12
			Total	97.9134	33.63109	12
		Ipsilat	Negative	97.7141	35.64642	12
			Positive	98.0728	32.94523	12
			Total	97.8935	33.56848	24
			Total	Average	94.3686	31.38181
			Negative	94.9706	34.28570	24
		Positive	93.8870	30.05376	24	
	Total	94.4087	31.50585	72		
Total	Contra	Average	86.0753	26.86897	28	
		Negative	89.3276	30.28639	28	
		Positive	83.4735	25.05804	28	
		Total	86.2921	27.26351	84	
	Ipsilat	Average	88.0954	28.60051	28	
		Total	88.0954	28.60051	28	
	Ipsilat	Negative	86.1748	31.35002	28	
		Positive	89.6320	27.74037	28	
		Total	87.9034	29.38176	56	
		Total	Average	87.0854	27.51372	56
		Negative	87.7512	30.58270	56	
		Positive	86.5527	26.37550	56	
	Total	87.1298	28.04817	168		

Appendix 16: Joint load statistics for dolichofacial subjects (Hypothesis 1)

D	F	Contra	Average	95.2998	27.72446	19		
			Negative	99.4607	30.10961	19		
			Positive	91.9711	26.22745	19		
			Total	95.5772	27.73315	57		
		Ipsilat	Average	82.3950	33.70569	19		
			Total	82.3950	33.70569	19		
		Ipsilat	Negative	79.2588	34.18309	19		
			Positive	84.9039	34.27607	19		
			Total	82.0814	33.88483	38		
			Total	Average	88.8474	31.13485	38	
		Total	Negative	89.3598	33.38085	38		
			Positive	88.4375	30.31527	38		
			Total	88.8816	31.35794	114		
			M		Contra	Average	112.4178	39.17149
		Contra	Negative	117.9744	43.57600	10		
			Positive	107.9726	35.99979	10		
Total	112.7883		38.53595	30				
Ipsilat	Average		106.4220	72.27542	10			
Ipsilat	Total	106.4220	72.27542	10				
	Negative	106.6839	78.71049	10				
Ipsilat	Positive	106.2124	68.56148	10				
	Total	106.4482	71.84240	20				
	Total	Average	109.4199	56.66292	20			
	Negative	112.3292	62.19039	20				
Total	Positive	107.0925	53.30421	20				
	Total	109.6139	56.56091	60				
	Total		Contra	Average	101.2026	32.49456	29	
	Contra	Negative	105.8447	35.68415	29			
Positive		97.4888	30.30986	29				
Total		101.5121	32.70001	87				
Ipsilat		Average	90.6802	50.44277	29			
Ipsilat	Total	90.6802	50.44277	29				
	Negative	88.7158	54.02333	29				
Ipsilat	Positive	92.2517	48.70766	29				
	Total	90.4837	51.01222	58				
	Total	Average	95.9414	42.38831	58			
	Negative	97.2803	46.19313	58				
Total	Positive	94.8703	40.29478	58				
	Total	96.0306	42.79005	174				

Appendix 17: Joint load overall statistics (Hypothesis 1 and 2)

Total	F	Contrn	Average	89.4548	26.77070	35	
			Negative	93.8343	29.37847	35	
			Positive	85.9513	25.21232	35	
			Total	89.7468	27.10671	105	
	Ipsilat	Average	81.6348	28.74496	35		
			Total	81.6348	28.74496	35	
	Ipsilat	Negative	78.4641	30.10842	35		
			Positive	84.1713	28.95807	35	
			Total	81.3177	29.46454	70	
	Total	Average	85.5448	27.85320	70		
			Negative	86.1492	30.52703	70	
			Positive	85.0613	26.96732	70	
			Total	85.5851	28.35626	210	
	M	Contrn	Average	100.6393	35.36262	22	
				Negative	103.9304	39.99076	22
				Positive	98.0064	32.29279	22
Total				100.8587	35.54677	66	
Ipsilat		Average	101.7809	53.38542	22		
			Total	101.7809	53.38542	22	
Ipsilat		Negative	101.7913	57.80685	22		
			Positive	101.7726	50.99334	22	
			Total	101.7820	53.86914	44	
Total		Average	101.2101	44.75391	44		
			Negative	102.8608	49.13415	44	
			Positive	99.8895	42.22368	44	
			Total	101.3201	45.12844	132	
Total		Contrn	Average	93.7716	30.56533	57	
				Negative	97.7311	33.88706	57
				Positive	90.6041	28.49654	57
	Total			94.0356	31.01732	171	
	Ipsilat	Average	89.4105	40.84512	57		
			Total	89.4105	40.84512	57	
	Ipsilat	Negative	87.4675	43.98595	57		
			Positive	90.9648	39.48400	57	
			Total	89.2162	41.64734	114	
	Total	Average	91.5911	35.98003	114		
			Negative	92.5993	39.42682	114	
			Positive	90.7845	34.27916	114	
			Total	91.6583	36.52467	342	

Appendix 18: Tests of Between-Subjects Effects (Hypothesis 1 and 2)

Tests of Between-Subjects Effects									
Source	Type III Sum of Squares	df	Mean Square	F	Sig.	Partial Eta Squared	Noncent. Parameter	Observed Power ^b	
Corrected Model	39275.134 ^a	23	1707.615	1.306	0.160	0.096	30.049	0.913	
Intercept	2610827.818	1	2610827.818	1997.523	0.000	0.863	1997.523	1.000	
DxGrp	7360.312	1	7360.312	5.631	0.018	0.017	5.631	0.658	
Sex	23228.247	1	23228.247	17.772	0.000	0.053	17.772	0.988	
Joint	1145.687	2	572.843	0.438	0.646	0.003	0.877	0.121	
LoadAngle	249.165	2	124.582	0.095	0.909	0.001	0.191	0.064	
DxGrp * Sex	1130.634	1	1130.634	0.865	0.353	0.003	0.865	0.153	
DxGrp * Joint	2996.529	2	1498.265	1.146	0.319	0.007	2.293	0.252	
DxGrp * LoadAngle	48.448	2	24.224	0.019	0.982	0.000	0.037	0.053	
Sex * Joint	1341.055	2	670.528	0.513	0.599	0.003	1.026	0.134	
Sex * LoadAngle	56.764	2	28.382	0.022	0.979	0.000	0.043	0.053	
Joint * LoadAngle	1318.902	1	1318.902	1.009	0.316	0.003	1.009	0.170	
DxGrp * Sex * Joint	25.545	2	12.773	0.010	0.990	0.000	0.020	0.051	
DxGrp * Sex * LoadAngle	68.789	2	34.395	0.026	0.974	0.000	0.053	0.054	
DxGrp * Joint * LoadAngle	26.729	1	26.729	0.020	0.886	0.000	0.020	0.052	
Sex * Joint * LoadAngle	184.745	1	184.745	0.141	0.707	0.000	0.141	0.066	
DxGrp * Sex * Joint * LoadAngle	48.923	1	48.923	0.037	0.847	0.000	0.037	0.054	
Error	415636.461	318	1307.033						
Total	3328135.238	342							
Corrected Total	454911.596	341							

a. R Squared = .086 (Adjusted R Squared = .020)

b. Computed using alpha = .05

Appendix 19: Female Joint Load Statistics (Hypothesis 2)

T-Test										
Sex = F, Joint = Contra, LoadAngle = Average										
Group Statistics ^a										
DxGrp		N	Mean	Std. Deviation	Std. Error Mean					
Load	B	16	82.5139	24.64580	6.16145					
	D	19	95.2998	27.72446	6.36043					
a. Sex = F, Joint = Contra, LoadAngle = Average										
Independent Samples Test ^a										
Levene's Test for Equality of Variances					t-test for Equality of Means					
		F	Sig.	t	df	Sig. (2-tailed)	Mean Difference	Std. Error Difference	95% Confidence Interval of the Difference	
Load	Equal variances assumed	0.526	0.474	-1.429	33	0.162	-12.78587	8.94750	-30.98970	5.41796
	Equal variances not assumed			-1.444	32.884	0.158	-12.78587	8.85542	-30.80478	5.23303
a. Sex = F, Joint = Contra, LoadAngle = Average										
Sex = F, Joint = Contra, LoadAngle = Negative										
Group Statistics ^a										
DxGrp		N	Mean	Std. Deviation	Std. Error Mean					
Load	B	16	87.1530	27.94150	6.98537					
	D	19	99.4607	30.10961	6.90762					
a. Sex = F, Joint = Contra, LoadAngle = Negative										
Independent Samples Test ^a										
Levene's Test for Equality of Variances					t-test for Equality of Means					
		F	Sig.	t	df	Sig. (2-tailed)	Mean Difference	Std. Error Difference	95% Confidence Interval of the Difference	
Load	Equal variances assumed	0.432	0.516	-1.245	33	0.222	-12.30773	9.88890	-32.42685	7.81138
	Equal variances not assumed			-1.253	32.657	0.219	-12.30773	9.82398	-32.30276	7.68730
a. Sex = F, Joint = Contra, LoadAngle = Negative										

Sex = F, Joint = Contra, LoadAngle = Positive

Group Statistics ^a					
DxGrp		N	Mean	Std. Deviation	Std. Error Mean
Load	B	16	78.8027	22.69287	5.67322
	D	19	91.9711	26.22745	6.01699

a. Sex = F, Joint = Contra, LoadAngle = Positive

Independent Samples Test ^a										
		Levene's Test for Equality of Variances				t-test for Equality of Means				
		F	Sig.	t	df	Sig. (2-tailed)	Mean Difference	Std. Error Difference	95% Confidence Interval of the Difference	
									Lower	Upper
Load	Equal variances assumed	0.531	0.472	-1.572	33	0.125	-13.16839	8.37542	-30.20831	3.87153
	Equal variances not assumed			-1.582	32.966	0.121	-13.16839	8.26980	-29.99408	3.65731

a. Sex = F, Joint = Contra, LoadAngle = Positive

Sex = F, Joint = Ipsilat, LoadAngle = Average

Group Statistics ^a					
DxGrp		N	Mean	Std. Deviation	Std. Error Mean
Load	B	16	80.7320	22.53874	5.63469
	D	19	82.3950	33.70569	7.73261

a. Sex = F, Joint = Ipsilat, LoadAngle = Average

Independent Samples Test ^a										
		Levene's Test for Equality of Variances				t-test for Equality of Means				
		F	Sig.	t	df	Sig. (2-tailed)	Mean Difference	Std. Error Difference	95% Confidence Interval of the Difference	
									Lower	Upper
Load	Equal variances assumed	4.216	0.048	-0.168	33	0.868	-1.66299	9.89591	-21.79636	18.47039
	Equal variances not assumed			-0.174	31.525	0.863	-1.66299	9.56781	-21.16351	17.83754

a. Sex = F, Joint = Ipsilat, LoadAngle = Average

Sex = F, Joint = Ipsilat, LoadAngle = Negative

Group Statistics ^a					
DxGrp		N	Mean	Std. Deviation	Std. Error Mean
Load	B	16	77.5202	25.51157	6.37789
	D	19	79.2588	34.18309	7.84214

a. Sex = F, Joint = Ipsilat, LoadAngle = Negative

Independent Samples Test ^a										
		Levene's Test for Equality of Variances				t-test for Equality of Means				
		F	Sig.	t	df	Sig. (2-tailed)	Mean Difference	Std. Error Difference	95% Confidence Interval of the Difference	
									Lower	Upper
Load	Equal variances assumed	3.794	0.060	-0.168	33	0.868	-1.73860	10.36532	-22.82700	19.34979
	Equal variances not assumed			-0.172	32.581	0.865	-1.73860	10.10825	-22.31403	18.83682

a. Sex = F, Joint = Ipsilat, LoadAngle = Negative

Sex = F, Joint = Ipsilat, LoadAngle = Positive

Group Statistics ^a					
DxGrp		N	Mean	Std. Deviation	Std. Error Mean
Load	B	16	83.3014	22.12357	5.53089
	D	19	84.9039	34.27607	7.86347

a. Sex = F, Joint = Ipsilat, LoadAngle = Positive

Independent Samples Test ^a										
		Levene's Test for Equality of Variances				t-test for Equality of Means				
		F	Sig.	t	df	Sig. (2-tailed)	Mean Difference	Std. Error Difference	95% Confidence Interval of the Difference	
									Lower	Upper
Load	Equal variances assumed	4.185	0.049	-0.161	33	0.873	-1.60250	9.96964	-21.88588	18.68088
	Equal variances not assumed			-0.167	31.086	0.869	-1.60250	9.61379	-21.20776	18.00276

a. Sex = F, Joint = Ipsilat, LoadAngle = Positive

Appendix 20: Male Joint Load Statistics (Hypothesis 2)

Sex = M, Joint = Contra, LoadAngle = Average											
Group Statistics^a											
DxGrp		N	Mean	Std. Deviation	Std. Error Mean						
Load	B	12	90.8238	30.01164	8.66362						
	D	10	112.4178	39.17149	12.38711						
a. Sex = M, Joint = Contra, LoadAngle = Average											
Independent Samples Test^a											
Levene's Test for Equality of Variances						t-test for Equality of Means					
		F	Sig.	t	df	Sig. (2-tailed)	Mean Difference	Std. Error Difference	95% Confidence Interval of the Difference		
Load	Equal variances assumed	0.129	0.724	-1.465	20	0.159	-21.59405	14.74479	-52.35115	9.16305	
	Equal variances not assumed			-1.429	16.691	0.172	-21.59405	15.11618	-53.53145	10.34335	
a. Sex = M, Joint = Contra, LoadAngle = Average											
Sex = M, Joint = Contra, LoadAngle = Negative											
Group Statistics^a											
DxGrp		N	Mean	Std. Deviation	Std. Error Mean						
Load	B	12	92.2270	34.21684	9.87755						
	D	10	117.9744	43.57600	13.77994						
a. Sex = M, Joint = Contra, LoadAngle = Negative											
Independent Samples Test^a											
Levene's Test for Equality of Variances						t-test for Equality of Means					
		F	Sig.	t	df	Sig. (2-tailed)	Mean Difference	Std. Error Difference	95% Confidence Interval of the Difference		
Load	Equal variances assumed	0.046	0.833	-1.553	20	0.136	-25.74734	16.57442	-60.32098	8.82630	
	Equal variances not assumed			-1.519	16.961	0.147	-25.74734	16.95443	-61.52433	10.02965	
a. Sex = M, Joint = Contra, LoadAngle = Negative											
Sex = M, Joint = Contra, LoadAngle = Positive											
Group Statistics^a											
DxGrp		N	Mean	Std. Deviation	Std. Error Mean						
Load	B	12	89.7012	27.65777	7.98411						
	D	10	107.9726	35.99979	11.38413						
a. Sex = M, Joint = Contra, LoadAngle = Positive											
Independent Samples Test^a											
Levene's Test for Equality of Variances						t-test for Equality of Means					
		F	Sig.	t	df	Sig. (2-tailed)	Mean Difference	Std. Error Difference	95% Confidence Interval of the Difference		
Load	Equal variances assumed	0.161	0.693	-1.347	20	0.193	-18.27142	13.56656	-46.57076	10.02792	
	Equal variances not assumed			-1.314	16.721	0.207	-18.27142	13.90484	-47.64537	11.10252	
a. Sex = M, Joint = Contra, LoadAngle = Positive											
Sex = M, Joint = Ipsialt, LoadAngle = Average											
Group Statistics^a											
DxGrp		N	Mean	Std. Deviation	Std. Error Mean						
Load	B	12	97.9134	33.63109	9.70846						
	D	10	106.4220	72.27542	22.85550						
a. Sex = M, Joint = Ipsialt, LoadAngle = Average											
Independent Samples Test^a											
Levene's Test for Equality of Variances						t-test for Equality of Means					
		F	Sig.	t	df	Sig. (2-tailed)	Mean Difference	Std. Error Difference	95% Confidence Interval of the Difference		
Load	Equal variances assumed	4.068	0.057	-0.364	20	0.719	-8.50960	23.34536	-57.20616	40.18897	
	Equal variances not assumed			-0.343	12.215	0.738	-8.50960	24.83199	-62.50722	45.49003	
a. Sex = M, Joint = Ipsialt, LoadAngle = Average											

Sex = M, Joint = Ipsilat, LoadAngle = Negative**Group Statistics^a**

DxGrp	N	Mean	Std. Deviation	Std. Error Mean
Load	B	12	97.7141	35.64642
	D	10	106.6839	78.71049

a. Sex = M, Joint = Ipsilat, LoadAngle = Negative

Independent Samples Test^a

		Levene's Test for Equality of Variances		t-test for Equality of Means						
		F	Sig.	t	df	Sig. (2-tailed)	Mean Difference	Std. Error Difference	95% Confidence Interval of the Difference	
									Lower	Upper
Load	Equal variances assumed	3.907	0.062	-0.355	20	0.726	-8.96982	25.28322	-61.70970	43.77005
	Equal variances not assumed			-0.333	12.051	0.745	-8.96982	26.93368	-67.62553	49.68589

a. Sex = M, Joint = Ipsilat, LoadAngle = Negative

Sex = M, Joint = Ipsilat, LoadAngle = Positive**Group Statistics^a**

DxGrp	N	Mean	Std. Deviation	Std. Error Mean
Load	B	12	98.0728	32.94523
	D	10	106.2124	68.56148

a. Sex = M, Joint = Ipsilat, LoadAngle = Positive

Independent Samples Test^a

		Levene's Test for Equality of Variances		t-test for Equality of Means						
		F	Sig.	t	df	Sig. (2-tailed)	Mean Difference	Std. Error Difference	95% Confidence Interval of the Difference	
									Lower	Upper
Load	Equal variances assumed	3.702	0.069	-0.365	20	0.719	-8.13961	22.29908	-54.65469	38.37546
	Equal variances not assumed			-0.344	12.420	0.737	-8.13961	23.67523	-59.53050	43.25127

a. Sex = M, Joint = Ipsilat, LoadAngle = Positive

Appendix 21: Joint Load T-Tests for males and females (Hypothesis 2)

T-Test										
Sex = F										
Group Statistics^a										
DxGrp		N	Mean	Std. Deviation	Std. Error Mean					
Load	B	96	81.6705	23.89166	2.43843					
	D	114	88.8816	31.35794	2.93694					
a. Sex = F										
Independent Samples Test^a										
		of Variances		t-test for Equality of Means						
		F	Sig.	t	df	Sig. (2-tailed)	Mean Difference	Std. Error Difference	of the Difference	
									Lower	Upper
Load	Equal variances assumed	12.030	0.001	-1.846	208	0.066	-7.21101	3.90555	-14.91055	0.48852
	Equal variances not assumed			-1.889	206.032	0.060	-7.21101	3.81727	-14.73694	0.31491
a. Sex = F										
Sex = M										
Group Statistics^a										
DxGrp		N	Mean	Std. Deviation	Std. Error Mean					
Load	B	72	94.4087	31.50585	3.71300					
	D	60	109.6139	56.56091	7.30198					
a. Sex = M										
Independent Samples Test^a										
		of Variances		t-test for Equality of Means						
		F	Sig.	t	df	Sig. (2-tailed)	Mean Difference	Std. Error Difference	of the Difference	
									Lower	Upper
Load	Equal variances assumed	9.769	0.002	-1.948	130	0.054	-15.20514	7.80570	-30.64779	0.23750
	Equal variances not assumed			-1.856	88.536	0.067	-15.20514	8.19178	-31.48322	1.07293
a. Sex = M										